AD-A263 382

Carderock Division
Naval Surface Warfare Center
Bethesda, Md. 20084–5000

CARDEROCKDIV–SSM–61–93/05 March 1993
Survivability, Structures, and Materials Directorate
Technical Report

Processing and Property Evaluation of Silver or Aluminum Matrix $YBa_2Cu_3O_{6+x}$ Superconducting Materials

by
A. Srinivasa Rao

DTIC
ELECTE
APR 22 1993
S D

93-08572
56pf

Approved for public release; distribution is unlimited.

93 4 21 043

CARDEROCKDIV–SSM–61–93/05 Processing and Property Evaluation of Silver or Aluminum Matrix YBa2Cu3O6+x Superconducting Materials

Carderock Division
Naval Surface Warfare Center
Bethesda, Md. 20084–5000

CARDEROCKDIV–SSM–61–93/05 March 1993
Survivability, Structures, and Materials Directorate
Technical Report

Processing and Property Evaluation of Silver or Aluminum Matrix $YBa_2Cu_3O_{6+x}$ Superconducting Materials

by

A. Srinivasa Rao

Approved for public release; distribution is unlimited.

CONTENTS

	Page
FIGURES	ii
ABSTRACT	1
ADMINISTRATIVE INFORMATION	2
INTRODUCTION	2
THEORETICAL	5
EXPERIMENTAL	8
RESULTS	14
Pure $YBa_2Cu_3O_{6+x}$ system	14
Silver/$YBa_2Cu_3O_{6+x}$ composite system	14
Aluminum/$YBa_2Cu_3O_{6+x}$ composite system	23
DISCUSSION	37
CONCLUSION	45
ACKNOWLEDGMENT	48
REFERENCES	48

DTIC QUALITY INSPECTED 4

Accession For	
NTIS GRA&I	☑
DTIC TAB	☐
Unannounced	☐
Justification	
By	
Distribution/	
Availability Codes	
Dist	Avail and/or Special
A-1	

FIGURES

Page

1. Flow diagram of the processing of aluminum / $YBa_2Cu_3O_{6+x}$ composites. 10

2. Typical extruded wires and tapes wound as long and flexible (A) coils or (B) tapes, and (C) hot pressed preform for small bar samples produced from 60 wt.% aluminum / 40 wt.% $YBa_2Cu_3O_{6+x}$ superconducting composites. 13

3. (A) $YBa_2Cu_3O_{6+x}$ particle morphology and (B) electrical resistance measured as a function of sample temperature of sintered $YBa_2Cu_3O_{6+x}$ ceramic material with 5 moles of excess CuO. 15

4. Electrical resistance versus temperature profiles of commercial silver/$YBa_2Cu_3O_{6+x}$ composites. Silver concentration (A) 100, (B) 10, (C) 20, (D) 30, (E) 40, (F) 50, (G) 60 and (H) 63.6 wt.%. 16

5. Zero resistance temperature versus silver concentration profile of silver/$YBa_2Cu_3O_{6+x}$ composites. 17

6. Typical microstructure of polished silver/$YBa_2Cu_3O_{6+x}$ composites. Silver concentration (A) 10, (B) 20, (C) 30, (D) 40, (E) 50 (F) 60 (G) 63.6 and (H) 72 wt.%. 19

7. Particle size versus silver concentration profiles of silver/$YBa_2Cu_3O_{6+x}$ composites. 20

8. Electrical resistance versus temperature profiles of commercial 1100 grade aluminum and aluminum/$YBa_2Cu_3O_{6+x}$ composites. Aluminum concentration (A) 100, (B) 10, (C) 20, (D) 30, (E) 40, (F) 50, (G) 55 and (H) 60 wt.%. 24

9. Cumulative plot of the electrical resistance versus temperature profile of 60 wt.% aluminum/40 wt.% $YBa_2Cu_3O_{6+x}$ composites. 25

10. Typical microstructure of polished aluminum/$YBa_2Cu_3O_{6+x}$ composites. Aluminum concentration (A) 10, (B) 20, (C) 40 and (D) 60 wt.%. 26

11. Electrical resistance versus temperature represented as a function of (actual) applied current for 60 wt.% aluminum/40 wt.% $YBa_2Cu_3O_{6+x}$ composites. 28

12. Transition temperature versus (actual) applied current plots of 60 wt.% aluminum/40 wt.% $YBa_2Cu_3O_{6+x}$ composites. . 29

Page

13. Magnetic moment versus sample temperature profiles of 60 wt.% aluminum/40 wt.% $YBa_2Cu_3O_{6+x}$ composites measured using SQUID. The applied magnetic field strengths are 35, 75 and 175 gauss. 31

14. Magnetic susceptibility versus sample temperature profiles of 60 wt.% aluminum/40 wt.% $YBa_2Cu_3O_{6+x}$ composites. 33

15. Electrical resistance versus temperature profiles of 60 wt.% aluminum/$YBa_2Cu_3O_{6+x}$ composites. 34

16. Electrical resistivity versus temperature profiles of 60 wt.% aluminum/$YBa_2Cu_3O_{6+x}$ composites measured using ac susceptibility method. 35

17. Electrical resistance versus temperature plots of 60 wt.% aluminum/40 wt. % $YBa_2Cu_3O_{6+x}$ composites represented as a function of (A, C) sintering temperature and (B) duration of sintering. Sintering temperature (A, B) 400°C and (C) 550°C. Duration of sintering (A, C) 30 and (B) 120 minutes.. 36

18. Electrical resistance versus applied current plots of 60 wt.% aluminum/40 wt.% $YBa_2Cu_3O_{6+x}$ composites measured using (A) small samples and (B) 50 cm long coil at 77K. 38

19. Typical microstructure representing two different regions of the polished surface of a long 60 wt.% aluminum/40 wt.% $YBa_2Cu_3O_{6+x}$ composite wire. Region (A) represents the uniform distribution of $YBa_2Cu_3O_{6+x}$ and the region (B) represents aggregation of $YBa_2Cu_3O_{6+x}$ particles.. 41

20. Typical microstructure and the corresponding compositional analysis of $YBa_2Cu_3O_{6+x}$-aluminum interface.... 43

21. The transmission electron micrographs obtained from the interfacial region between aluminum matrix and $YBa_2Cu_3O_{6+x}$ particle. 44

Figure 22. Schematic representation of the material electrical property as a function of silver concentration for silver / $YBa_2Cu_3O_{6+x}$ composites. 46

Figure 23. Schematic representation of the material electrical property as a function of aluminum concentration for aluminum / $YBa_2Cu_3O_{6+x}$ composites. 47

ABSTRACT

In order to understand (a) the physical behavior at the atomistic level of the superconducting metal matrix composites, (b) to develop an analytical model and derive solutions for explaining the superconducting behavior of metal based composite systems and (c) to develop a process to produce very ductile new metal matrix superconducting wires and tapes with acceptable superconducting temperature (T_c) and current carrying capacity (J_c) two metal matrix composite systems (aluminum/$YBa_2Cu_3O_{6+x}$ and silver/$YBa_2Cu_3O_{6+x}$) have been investigated. The composites that were processed contain 10 - 72 wt.% aluminum or silver and the processing procedures were similar to those used in conventional powder metallurgy.

The results suggest that silver forms superconducting composites in the concentration range 10- 72 wt.%. However, three superconducting transition temperatures were observed for composites containing different amounts of silver (viz. 1 - 10 wt.% silver $T_c \leq 86$ K; 10 - 40 wt.% silver T_c range 86 - 77 K and 40 - 72 wt.% silver T_c range 77 - 60 K respectively). The superconducting behavior of silver composites can be explained in terms of the proximity effect, however, the estimated extrapolation length for the diffusion of superconducting electrons into the silver matrix is much less than the superconducting particle - particle separation distance measured from the experimentally determined values. The critical current value (J_c) measured at liquid nitrogen temperature (~77 K) was found to depend upon the concentration of silver in the composite and the absolute value for composites containing 10 and 40 wt.% silver was 100 and 25 amp cm^{-2} respectively.

The most intriguing and new discovery is the production of aluminum based composites that can superconduct around 90 K. The results indicate that the 10 - 55 wt.% aluminum composites do not show any superconducting behavior. However, the 60 wt.% aluminum/40 wt.% $YBa_2Cu_3O_{6+x}$ composites show a zero resistance transition around 90 K and very interesting second transition around 120 K suggesting that a new generation of metal matrix superconducting composites has been discovered. For the aluminum concentrations $\geq$ 62 wt.%, the composite electrical resistance versus temperature behavior is similar to that of pure aluminum conductor. Since the superconducting behavior of the aluminum composites was limited to a narrow concentration range, no current theories of superconductivity were found to be applicable to this system and it is possible that the mechanism of the observed "anomaly" may be explained in

terms of the electronic charge density structure of aluminum/$YBa_2Cu_3O_{6+x}$ interface. In addition it was found that the superconducting behavior of the 60 wt.% aluminum/40 wt.% $YBa_2Cu_3O_{6+x}$ composites is very sensitive to the sintering temperature and the duration of sintering. The critical current values measured at the liquid nitrogen temperature and zero magnetic field were found to be 50 amp cm^{-2} and 10 - 15 amp cm^{-2} for small samples and 50 cm long coils respectively. The microstructural examination of the samples revealed that the extrusion process, that was used to produce long wires or tapes tends to introduce an uneven distribution of superconducting $YBa_2Cu_3O_{6+x}$ particles in the aluminum matrix. It is possible that such an uneven distribution of $YBa_2Cu_3O_{6+x}$ has resulted in the lowering of critical current from 50 amp cm^{-2} to 10 - 15 amp cm^{-2}.

ADMINISTRATIVE INFORMATION

This report was funded by the CDNSWC Independent Research Program, sponsored by the Office of the Naval Research, ONR 10, and administered by the Research Director, CDNSWC 0112, Dr. Bruce Douglas, under program element 61152N, Task Area ZR-000-01-01 and CDNSWC Work Unit 1-2812-148. This work was supervised within the Metals and Welding Division (Code 281) by Dr. O. P. Arora.

INTRODUCTION

The electrical systems that are presently being used in superconducting magnet or motor generator applications must be cooled with liquid helium (temperature ~ 4 K). In order to maintain the superconductor temperature at 4K, a special and more complicated cryogenic system is required to maintain liquid helium state of the coolant. Ceramic superconductors have now been identified that they can superconduct at liquid nitrogen temperatures (temperature ~ 77 K) and somewhat higher [1-3]. The ability to cool a superconductor with liquid nitrogen versus liquid helium offers logistical

advantages for the Navy in both system reliability and operational cost. However, the new high temperature superconducting ceramic materials generally are very hard and brittle, and are very difficult to be processed into useful net shaped components. New processes to enhance the ease of fabrication of these materials into useful shapes, such as wires for magnets as used in the electric drive system motors and generators, are being sought to reduce the overall cost of the system. Such process would be used to produce net shaped objects such as low loss microwave cavities or hollow tube "down leads" that will transition the current leads from room temperature to that of a helium cooled superconducting storage magnet.

In the open literature there have been many claims of processing the yttrium based $YBa_2Cu_3O_{6+x}$ ceramic materials into useful components, however, to date no flexible superconducting components have been produced. Recently it has been recognized that the key to achieving more flexibility of the final superconductor is to incorporate highly ductile metallic species such as silver or gold during the initial phase of processing [4-5]. However, composite processing based on either gold or silver is not economical for large scale manufacturing. Some researchers have suggested that aluminum can be a suitable alternative for either silver or gold, provided that the superconducting composite processing involves steps to prevent the formation of aluminum oxide [6-8]. Although a few investigators have reported that they have succeeded in overcoming the problem associated with the aluminum oxide formation, others have concluded that the addition of even a small percentage

of aluminum will lower the superconducting transition temperature (T_c) significantly [9-11]. These researchers have indicated that if the concentration of aluminum in the composite is above 10 wt.%, the metallic additive (aluminum) would destroy the superconducting property of the $YBa_2Cu_3O_{6+x}$ completely. At CDNSWC, Annapolis, under a separate program entitled "Superplasticity in Ceramic Superconductors," a detailed and thorough basic scientific investigation was carried out. Most of the effort under that program was focused to understand the effect of alumina or silver oxide on $YBa_2Cu_3O_{6+x}$ particle structure, morphology, superconductivity and deformation behavior. During that investigation, aluminum powder was used instead of alumina. An accidental explosion of the samples containing aluminum inside the sintering furnace has produced very flexible aluminum rich composite. When the electrical resistance versus temperature profile of the explosion induced composite was determined, it was found that the sample behaved as a superconductor with two transitions around ~ 90 and ~ 120 K indicating that a new aluminum based superconducting material system has been discovered. In order to obtain a similar composites, few experiments were conducted on aluminum/$YBa_2Cu_3O_{6+x}$ powder compacts. The experiments were so designed that the processing would simulate the sintering conditions that has led to the original discovery of the new materials. The simulated processing experiments have demonstrated that a new breed of aluminum metal based superconducting composites can be produced provided the $YBa_2Cu_3O_{6+x}$ can be incorporated into the matrix of aluminum without any structural degradation (i.e., without the conversion of superconducting orthorhombic phase to non -

superconducting tetragonal phase). As a result a new program on the superconducting metal matrix composite materials has been initiated under the Independent Research Program.

The over all goal of this project can be summarized as follows : (a) to understand the basic physics of the superconducting behavior of aluminum/$YBa_2Cu_3O_{6+x}$ composites, (b) to establish processing criteria for producing aluminum based composites without any structural degradation and (c) to produce strong and flexible wires and tapes with optimized superconducting properties (viz. T_c and J_c). This paper describes the basic structural, microstructural and superconducting properties of aluminum/$YBa_2Cu_3O_{6+x}$ composites as a function of processing methodology. The results obtained from a similar study on sliver/$YBa_2Cu_3O_{6+x}$ composites are also discussed for comparison.

THEORETICAL

Although the high temperature superconducting materials have been established during the past five years, the actual mechanism of the superconducting behavior of these materials, in particular in composite systems, has not been understood. The behavior of composites in low temperature superconductors has been explained in terms of the diffusion of "Cooper pairs" from superconducting material into the non superconducting metallic conductor.

In general it has been suggested that if a normal metal is deposited on top of a superconducting material with a good electrical contact, the composite system can show some

superconducting property due to the leakage of "Cooper pairs" from superconductor into the metal. Such an effect is often called the "proximity effect" and the typical distance of diffusion in classical metallic superconductors is given as 0.1 micron. Deutscher and de Gennes [13] has suggested that the superconducting transition temperature of the composite system (T_{cc}) can be related to the T_{cs} of the pure superconductor and the extrapolated length of diffusion of superconductivity from superconductor to the metal as

$$T_{cc} = T_{cs} - A\ (1/D_s+B)^2 \quad \ldots\ldots(1)$$

where A is a constant, D_s is the thickness of the superconducting layer and B is the extrapolation length for the diffusion of superconductivity from a superconductor to the metal.

Pande [14] suggested that the superconductivity of a composite can be expressed as a function of superconductor concentration of the composite empirically as

$$\ln\ [T_{cc} / T_{cs}] = (Q_o + Q\ (1-f_v/f_v))^{-1} \quad \ldots.(2)$$

where Q_o and Q are constants which represents the extrapolation length of the diffusion of superconductivity, and $(1-f_v)$ and f_v volume fraction of the superconducting and non - superconducting phases respectively. The above equation thus will provide a relationship between the concentration of the superconducting phase (i.e. $YBa_2Cu_3O_{6+X}$) and the superconducting transition temperature (T_c) of the composite. However, Pande's equation cannot provide a direct estimate of the extrapolated length of the diffusion of the superconductivity from the superconductor to the metal.

As a first attempt a new mathematical expression was derived to explain the superconductivity of the metal matrix composite system as a function of the extrapolated length of diffusion of superconductivity into the metal matrix. It was assumed that the process of the diffusion of superconducting electrons from the superconductor through the non-superconducting metal matrix is similar to that of the diffusion of the electric charge from a polarized oxide surface into the liquid phase and form an electrical double layer at a solid - liquid interface.

In this approach, it was assumed that that the penetration of the superconducting electrons into the non-superconducting metal matrix constitutes two different regions. In the first region, the electrons form a fixed boundary which is formed due to the leakage of the "Cooper Pairs", a process similar to that of the diffusion in low temperature superconductors (typical distance ~ 0.1 micron). The second region constitutes the superconducting electron diffusion into the metal. Assuming that the electron distribution in the diffused boundary follows Poisson - Boltzmann equation, the superconductivity of the composite can be represented as a function of concentration of the superconducting phase and the extrapolation length for the diffusion of the superconductivity in the simplified final form as

$$(T_{cc} / T_{cs}) = A \exp (- CB) \qquad .....(3)$$

where A is a constant that represents the "Cooper Pair" leakage distance into the non-superconducting metal
$C = ((1 - f_v) / f_v)$ where
$1-f_v$ is the volume fraction of the superconducting phase f_v is the

volume fraction of the non superconducting phase and
B is the diffusional distance for the superconducting electrons into the metal.

Although, the final form of the new solution is similar to that of the mathematical expression that was suggested by Pande, the new equation (equation 3) will enable to determine the extrapolation length for the diffusion of the superconductivity into non-superconducting metal directly.

The above three expressions not only can be applied to test the validity of the proximity theory of low temperature superconductors for high superconducting metal matrix composites, but also can be used for the determination of the extrapolated length of the diffusion of superconductivity from the superconductor to the metal matrix from the information of the superconducting transition temperature of a composite (T_{CC}) measured as a function of composite composition.

EXPERIMENTAL

The basic superconducting ceramic powder, $YBa_2Cu_3O_{6+x}$, was prepared by solid state chemical reaction. The superconducting transition temperature of the sintered $YBa_2Cu_3O_{6+x}$ was found to be 88 ± 2 K. Preliminary investigations on aluminum/pure $YBa_2Cu_3O_{6+x}$ composites indicated that 60 wt.% aluminum/40 wt.% $YBa_2Cu_3O_{6+x}$ composites behave as superconducting materials below 75 ± 10 K. However, it was found that an addition of excess copper oxide during the synthesis of $YBa_2Cu_3O_{6+x}$ has improved the superconducting properties of final aluminum composites [12]. Therefore, during the synthesis of the superconducting $YBa_2Cu_3O_{6+x}$ powder, nearly 5 moles

of excess copper oxide were added to the precursors. Based on the microstructural characterization, it has found that the excess (5 moles) copper oxide did not participate in the chemical reaction between 1 mole of Y_2O_3, 2 moles of $BaCO_3$ and 3 moles of CuO to form 1 mole of $YBa_2Cu_3O_{6+x}$ but remained as CuO. However, a small amount (< 10 %) of the excess CuO was reduced to metallic copper during the chemical reaction.

Figure 1 shows a typical flow diagram of the processing of aluminum/$YBa_2Cu_3O_{6+x}$ composite processing. The aluminum and silver composites were produced in two separate processing steps. In the first processing step, the superconducting $YBa_2Cu_3O_{6+x}$ with an excess (5 moles) of CuO was synthesized from Y_2O_3, $BaCO_3$ and CuO powders via solid state chemical reaction method. The details of the powder synthesis were given elsewhere [15]. The as-synthesized Y-Ba-Cu-O powder containing 5 moles of excess CuO was ground into a fine powder using mortar and pestle and the powder characteristics are given in Table 1.

Table 1. As - synthesized yttrium, barium and copper oxide ($YBa_2Cu_3O_{6+x}$) powder characteristics.

Density (gm / c.c)	6.0
Average particle size (micron)	~10.0
Surface area (m^2 / gm)	0.22

In the second processing step, commercially available fine (99.9 % pure) aluminum or silver powder was then added to Y-Ba-Cu-O powder and were mixed thoroughly in dry state in a ball mill using zirconia balls for one hour. Two sets of experimental procedures were

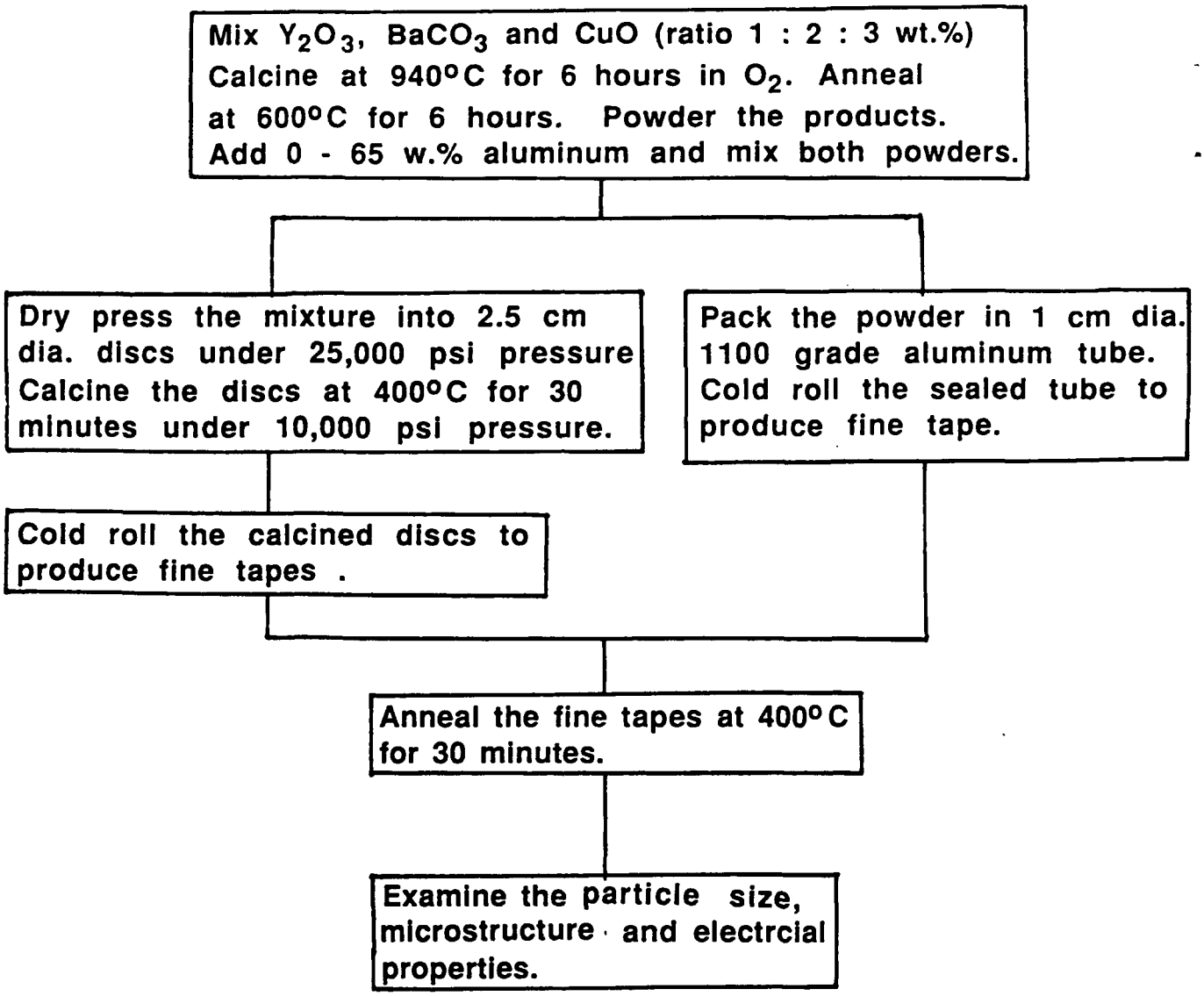

Figure 1. Flow diagram of the processing of aluminum / $YBa_2Cu_3O_{6+x}$ composites.

adopted for producing final composites. In the first set of experiments, the powder mixture (aluminum or silver powder and $YBa_2Cu_3O_{6+x}$ powder) was dry pressed into small 2.5 cm diameter discs under an applied pressure of 25,000 psi. The cold pressed discs were placed between two thick aluminum or silver plates. While aluminum composites were sintered at 400°C for 30 minutes, the silver composites were sintered at 700°C for 30 minutes. During sintering the composite sample was also subjected to a constant axial load of 10,000 psi. The sintered discs were cooled in nitrogen and were cut into small 2 X 2 X 25 mm bars. In the second set of experiments, the mixture containing aluminum and $YBa_2Cu_3O_{6+x}$ powders was introduced into a commercial 1100 aluminum tube. After closing both ends of the tube with plugs of the same 1100 series aluminum, the tube was subjected to cold rolling process in order to produce fine wires (2 mm in diameter) and 0.02 mm thick tapes. Due care was taken in order to prevent the heating of the aluminum tube during the cold rolling process. The final aluminum composite wires and tapes were annealed at 400°C for 30 minutes in flowing nitrogen gas atmosphere. It has to be pointed out that the sintering and annealing temperature for aluminum and silver composites were chosen to be different because, the preliminary experimental results indicated that a better composite density and adhesion at the metal matrix and the superconducting ceramic interface can be achieved only when the composites are processed at a temperature with in 250 - 300°C of the melting temperature of the matrix material. Figure 2 shows typical aluminum/$YBa_2Cu_3O_{6+x}$ coils and tapes that were extruded using the cold rolling process. The pre-form from which

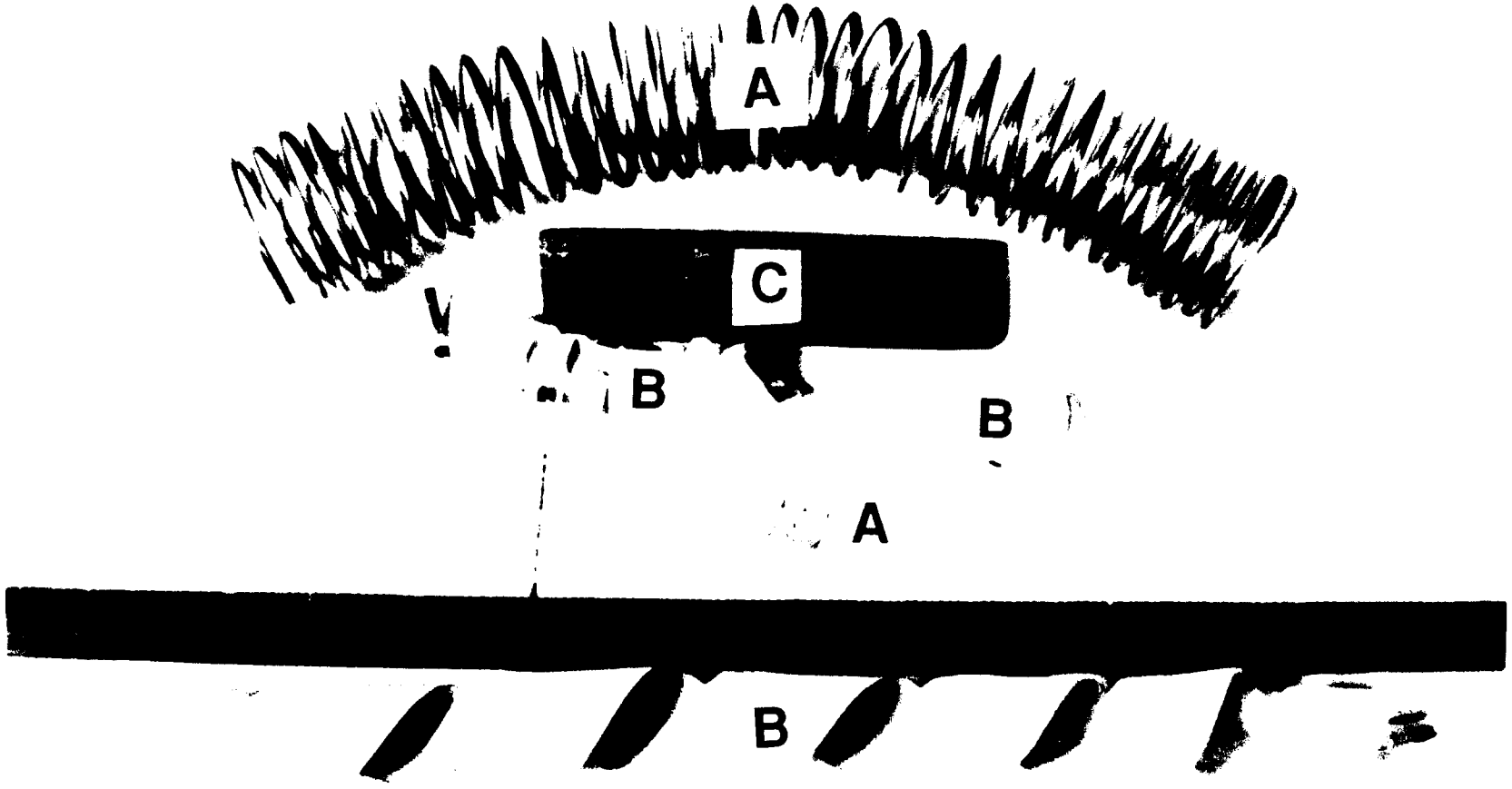

Figure 2. Typical extruded wires and tapes wound as long and flexible (A) coils or (B) tapes, and (C) hot pressed pre-form for small bar samples produced from 60 wt.% aluminum / 40 wt.% $YBa_2Cu_3O_{6+x}$ superconducting composites.

the small test samples (2 X 2 X 25 mm bars) were cut are also shown in Figure 2 for comparison.

The microstructure of all samples (obtained from small bars, 2 mm dia. wires and 0.02 mm thick tapes) were examined under both optical, scanning and transmission electron microscopes. The structural characterization of the superconducting $YBa_2Cu_3O_{6+x}$ particles was carried out using x-ray diffraction. The electrical resistance of all samples was measured as a function of temperature using a dc four probe resistivity measurement unit. Since the four probe measurement unit cannot accommodate large samples the electrical resistance, measurements of the composites were made on small samples. In order to obtain a representative measurement of the resistance of long wires or tapes, small samples were cut from various positions along the length of the wires or tapes and the electrical resistance of all small samples (that represent the entire length of the long wire or tape) was measured as a function of temperature. The final comparison of the resistance of the long coil and the sum total of small samples was made by normalizing the resistance value in terms of electrical resistivity (which is given as sample resistance X area of cross section / total length of the sample). In addition, some coils were produced from 50 cm long and 2 mm dia. wires and/or 0.02 mm tapes and the electrical resistance of these coils was measured as a function of applied current at liquid nitrogen (~77 K), dry ice (~250 K), ice (~273 K) and room temperature (~ 293 K).

RESULTS

Pure $YBa_2Cu_3O_{6+x}$ System

Figure 3A shows a typical morphology of sintered superconducting ceramic material processed using the as-synthesized $YBa_2Cu_3O_{6+x}$ powder containing 5 moles of excess CuO. The electrical resistance versus temperature behavior of the same sample is shown in Figure 3B. The results shown in Figures 3 (A) and (B) suggest that the $YBa_2Cu_3O_{6+x}$ particles tend to sinter into long elongated rods/plates and the sintered ceramic shows superconducting transition around 86 K. The electrical resistance versus temperature results also indicate that the presence of excess 5 moles of CuO has no effect on the superconducting property of pure $YBa_2Cu_3O_{6+x}$ (pure $YBa_2Cu_3O_{6+x}$ has a T_c 86$\pm$2 K). The X - ray diffraction patterns obtained from the above samples indicated that the sintered ceramic contains copper, but, the primary crystal structure of the sintered material represents the orthorhombic (superconducting) structure of pure $YBa_2Cu_3O_{6+x}$ material that has been reported in the literature.

Silver/$YBa_2Cu_3O_{6+x}$ Composite System

Figure 4 shows typical electrical resistance versus temperature plots of pure silver and silver/$YBa_2Cu_3O_{6+x}$ composites. The zero resistance temperature versus silver concentration in the composites was determined from a number of resistance versus temperature plots similar to those shown in Figure 4 and the results are shown in Figure 5. The results indicate that the silver composites show superconducting behavior throughout the entire concentration range

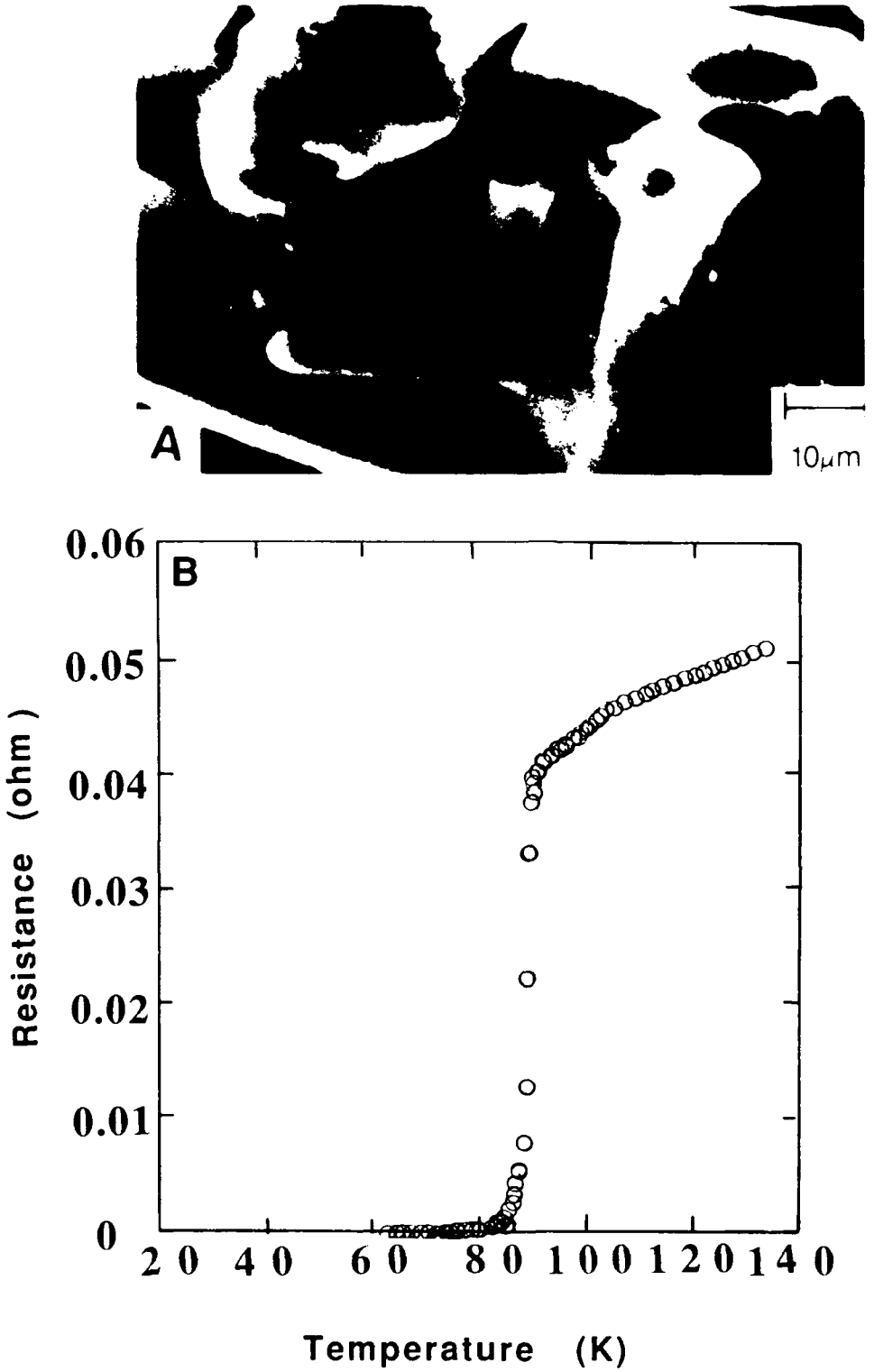

Figure 3. (A) $YBa_2Cu_3O_{6+x}$ particle morphology and (B) electrical resistance measured as a function of sample temperature of sintered $YBa_2Cu_3O_{6+x}$ ceramic material with 5 moles of excess CuO.

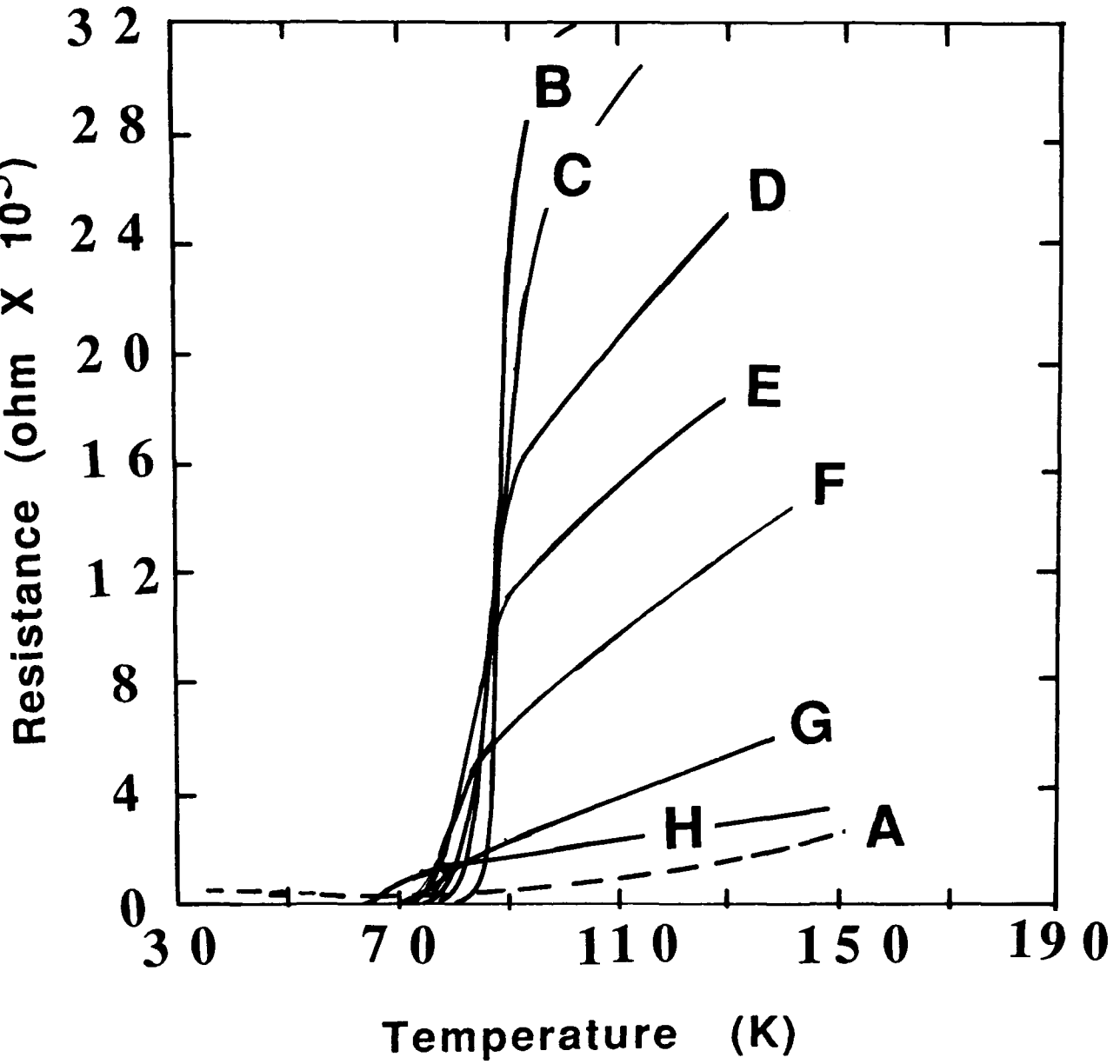

Figure 4. Electrical resistance versus temperature profiles of commercial silver / $YBa_2Cu_3O_{6+x}$ composites. Silver concentration (A) 100, (B) 10, (C) 20, (D) 30, (E) 40, (F) 50, (G) 60 and (H) 63.6 wt.%.

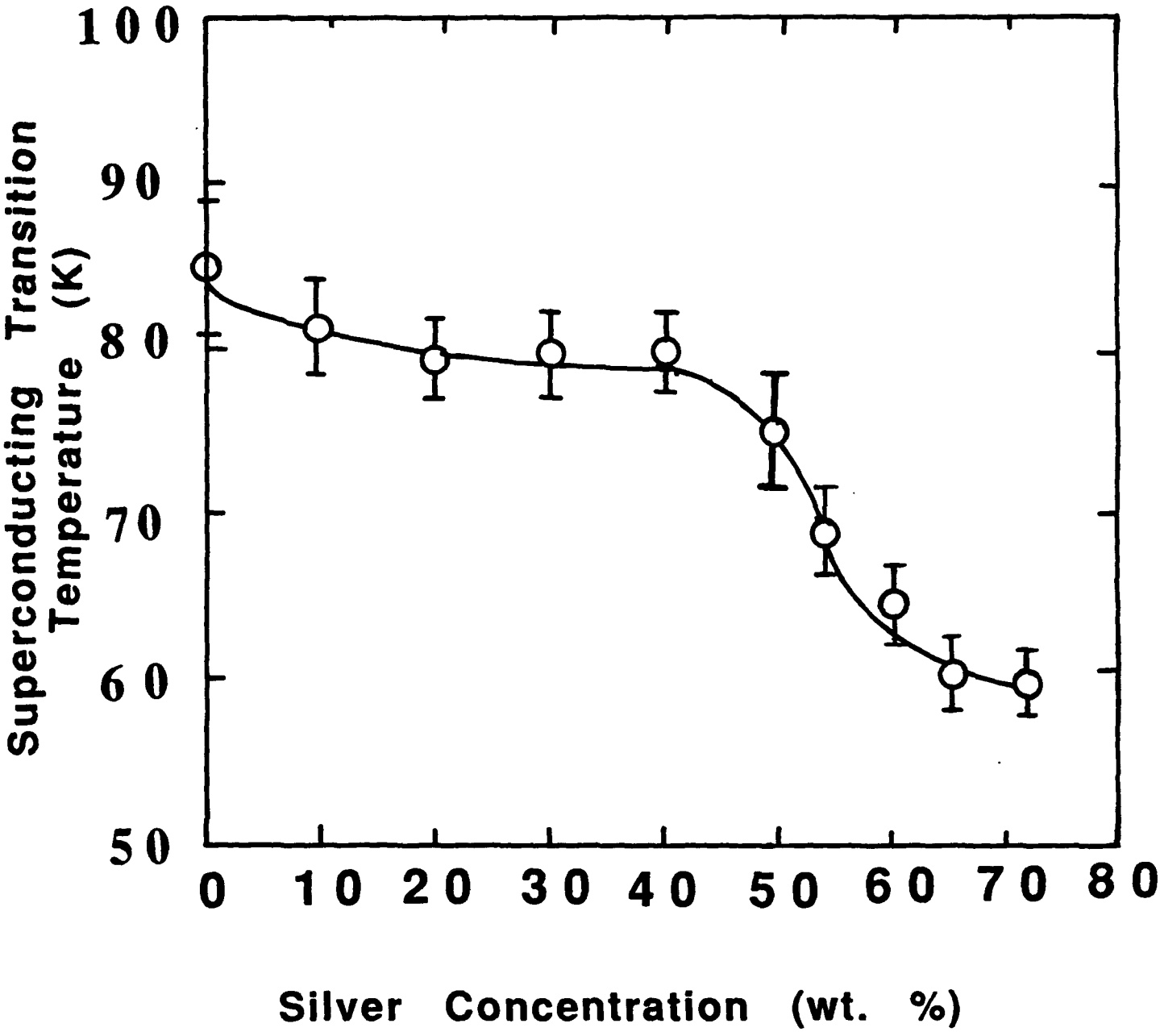

Figure 5. Zero resistance temperature versus silver concentration profile of silver / $YBa_2Cu_3O_{6+x}$ composites.

investigated (10 - 72 wt.% silver). However, the zero resistance temperature (T_c) tends to decrease with an increase in the concentration of silver in the range 0 - 10 wt.% and 40 - 72 wt.%. The T_c remains nearly independent of silver concentration in the range 10 - 40 wt.%. In addition, the results also suggest that the normal state resistance of the composites decreases with an increase in the silver concentration.

The typical microstructure of silver composites obtained from polished sample surfaces is shown as a function of silver concentration in Figure 6. The results suggest that the distribution of $YBa_2Cu_3O_{6+x}$ in silver matrix is very uniform and the degree of uniformity increases with an increase in the concentration of silver in the composites. In order to model the superconducting property of the composites in terms of the separation distance between two $YBa_2Cu_3O_{6+x}$ particles, a number of photomicrograhs representing the microstructure of all composites were obtained. From the micrographs the average particle size was estimated (Figure 7). From Figure 7 it can be noticed that the particle size of $YBa_2Cu_3O_{6+x}$ increases with an increase in the silver concentration initially in the range 0 - 10 wt.%. For the silver concentration above 10 wt.% this trend is reversed. Assuming that the particles are spherical, the $YBa_2Cu_3O_{6+x}$ particle - particle separation distance was estimated as a function of silver concentration. The results indicate that the separation distance increases with an increase in the silver concentration. Typical value of the $YBa_2Cu_3O_{6+x}$ particle - particle separation distance for 10 wt.% and 72 wt.% silver composites was found to be 1 and 37

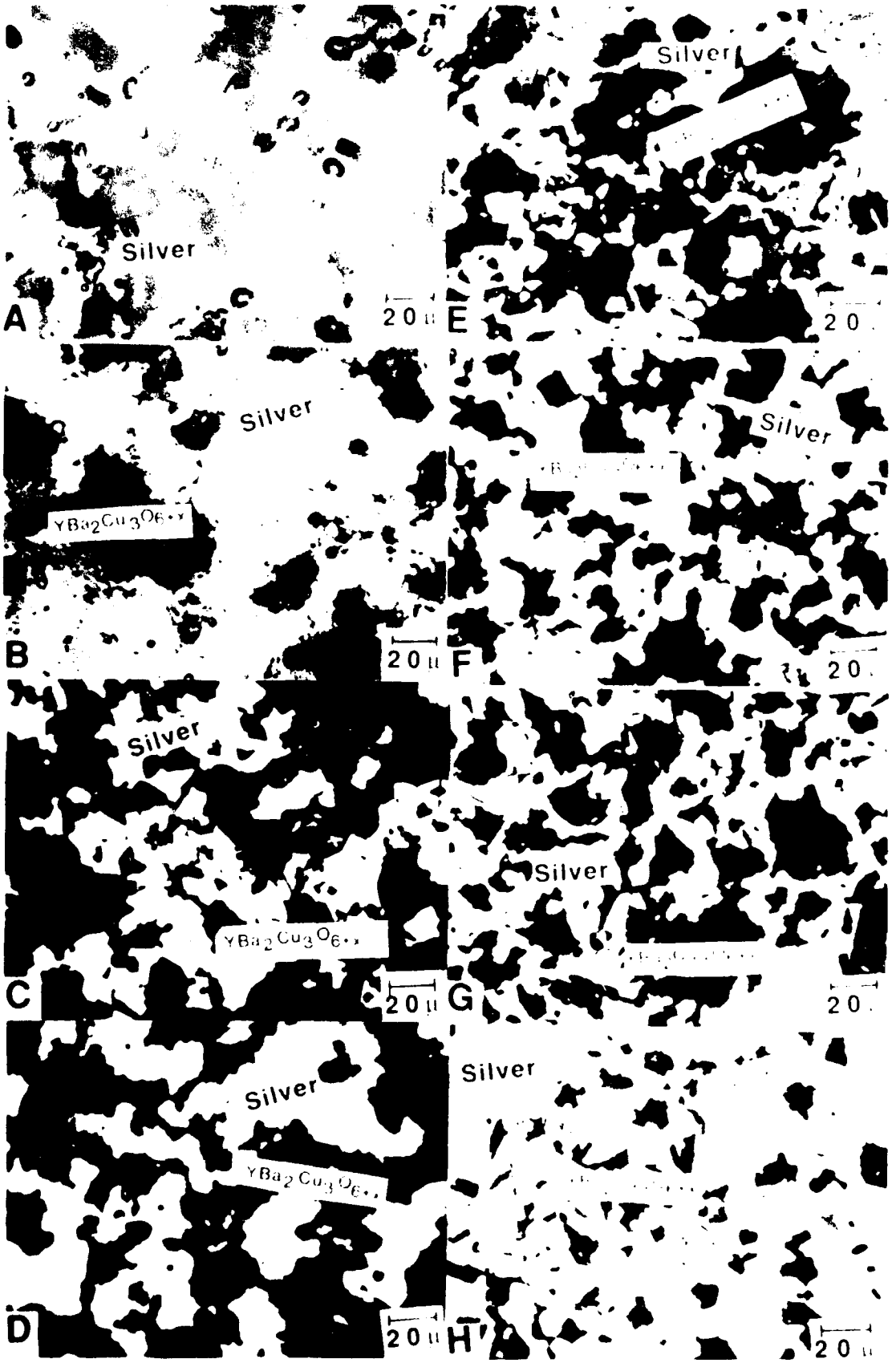

Figure 6. Typical microstructure of polished silver/ $YBa_2Cu_3O_{6+x}$ composites. Silver concentration (A) 10, (B) 20, (C) 30, (D) 40, (E) 50 (F) 60 (G) 63.6 and (H) 72 wt.%.

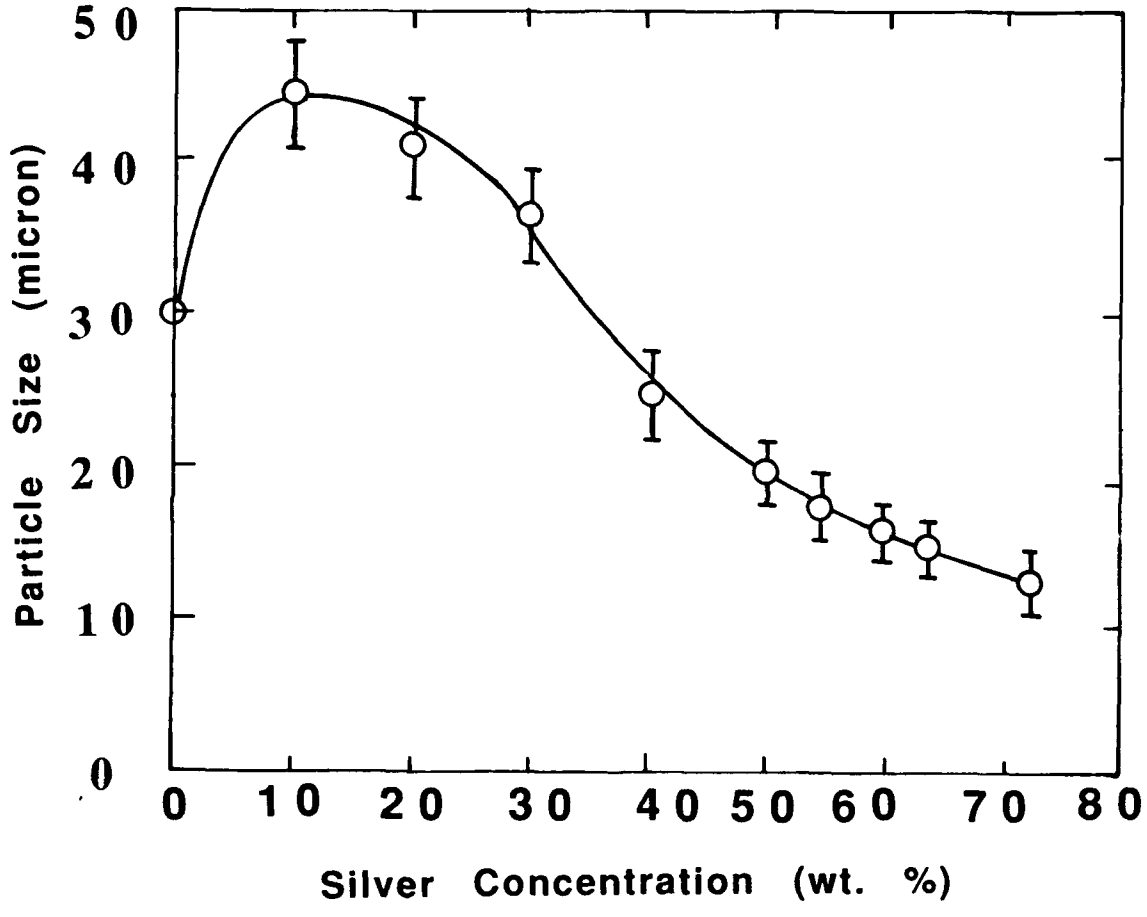

Figure 7. Particle size versus silver concentration profiles of silver / $YBa_2Cu_3O_{6+x}$ composites.

microns respectively.

The critical current density measured at the liquid nitrogen temperature (~77 K) of the silver composites containing silver 10 and 40 wt.% was found to be 100 and 25 amp/cm^{-2} respectively. These values are lower than those reported in the literature for bulk silver composites [16]. It is thought that such a low value for the J_c is perhaps due to the fact that the composites are not dense enough to overcome the weak links at the interface between the silver matrix and the superconducting $YBa_2Cu_3O_{6+x}$ particles.

In order to understand the mechanism of the superconducting behavior of the silver composites, the proximity theory was applied. According to the classical proximity theory of low temperature superconductors, the extrapolated length for the diffusion of "Cooper pairs" from superconductor to the non superconducting metallic conductor is ~ 0.1 microns. However, the measured separation distance for the silver superconductors range from 1 - 37 microns. It is therefore, evident from the measured separation distance data that the proximity theory of low temperature superconductors is not applicable to the high temperature superconducting silver composite system to predict the extrapolated length of the diffusion of superconductivity. An effort was made to estimate the extrapolated length of diffusion of the superconducting electrons into the silver matrix using the above suggested Deutscher and de Gennes model, Pande model and the model that was developed during the present investigation (Equations 1 - 3). The results of the modeling indicated that the present data on silver composites

can be normalized on the Deutscher and de Gennes's expression (equation 1), over the entire concentration range investigated (i.e. silver concentration range 10 - 72 wt.%). However, the model predicts that the maximum distance that the superconducting electrons can penetrate into the matrix will be ~ 6 microns. A similar analytical treatment of the measured data with the other two models (equations 2, and 3) reveal that the over all behavior of the silver composites (over the concentration range 10 - 72 wt.%) cannot be normalized into one generalized expression. Analytical treatment of the experimental results using the equations 2 and 3 suggested that the observed superconducting behavior of silver composites fall into two categories (viz. composites containing 10 - 40 wt.% silver; and $T_c \geq 60$ K) and composites containing 40 - 72 wt.% silver; and $T_c \leq 60$ K). In addition, the present model predicted the diffusional depth for superconducting electrons to range from 0.28 - 2 microns. These results indicate that the predicted extrapolated lengths for the diffusion of superconductivity are too low compared to the measured separation distance (range 1 - 37 micron).

The above disagreement may arise due to several factors. For example, (1) the above models assume that the superconducting phenomena in these materials is similar to that of low temperature (liquid helium temperature) superconductors; (2) the separation distances were estimated taking into consideration only the large superconducting $YBa_2Cu_3O_{6+x}$ particles that were accessible for the estimation of particle size (it is possible that a large fraction of very fine (<0.1 micron) size particles that are often distributed throughout the matrix may account for smaller separation distance

between any two adjacent superconducting $YBa_2Cu_3O_{6+x}$ particles); and (3) the model does not take into account the three dimensional effect of the particle particle separation.

Aluminum/$YBa_2Cu_3O_{6+x}$ Composite System

Figure 8 shows typical electrical resistance versus temperature plots of pure aluminum and aluminum/$YBa_2Cu_3O_{6+x}$ composites. The results indicate that the aluminum composites show typical metallic behavior (and composite resistance >> resistance of pure aluminum) when the aluminum concentration is in the range of 10 - 55 wt.%. In addition, the results also suggest that the resistance of the composites decreases with an increase in the aluminum concentration. However, if the concentration of the aluminum in the composites is ~ 60 wt.%, unlike for pure $YBa_2Cu_3O_{6+x}$ system, the new aluminum composite system shows two transitions of the electrical resistance around 90 and 120 K. Above the concentration range of $\geq$ 62 wt.%, the aluminum composites behave as normal metallic conductors with electrical resistance versus temperature behavior similar to that of pure aluminum (and composite resistance ~ resistance of pure aluminum). From a number of electrical resistance measurements a cumulative resistance versus temperature plot for 60 wt.% aluminum/40 wt.% $YBa_2Cu_3O_{6+x}$ composite was developed. The results are shown in Figure 9 and the results suggest that the 60 wt.% aluminum/40 wt.% $YBa_2Cu_3O_{6+x}$ composite shows a broad transitional regions around 90 and 120 K. The typical microstructure of aluminum composites obtained from polished sample surfaces is shown as a function of aluminum concentration in Figure 10. The results indicate that the distribution of $YBa_2Cu_3O_{6+x}$ in aluminum matrix is

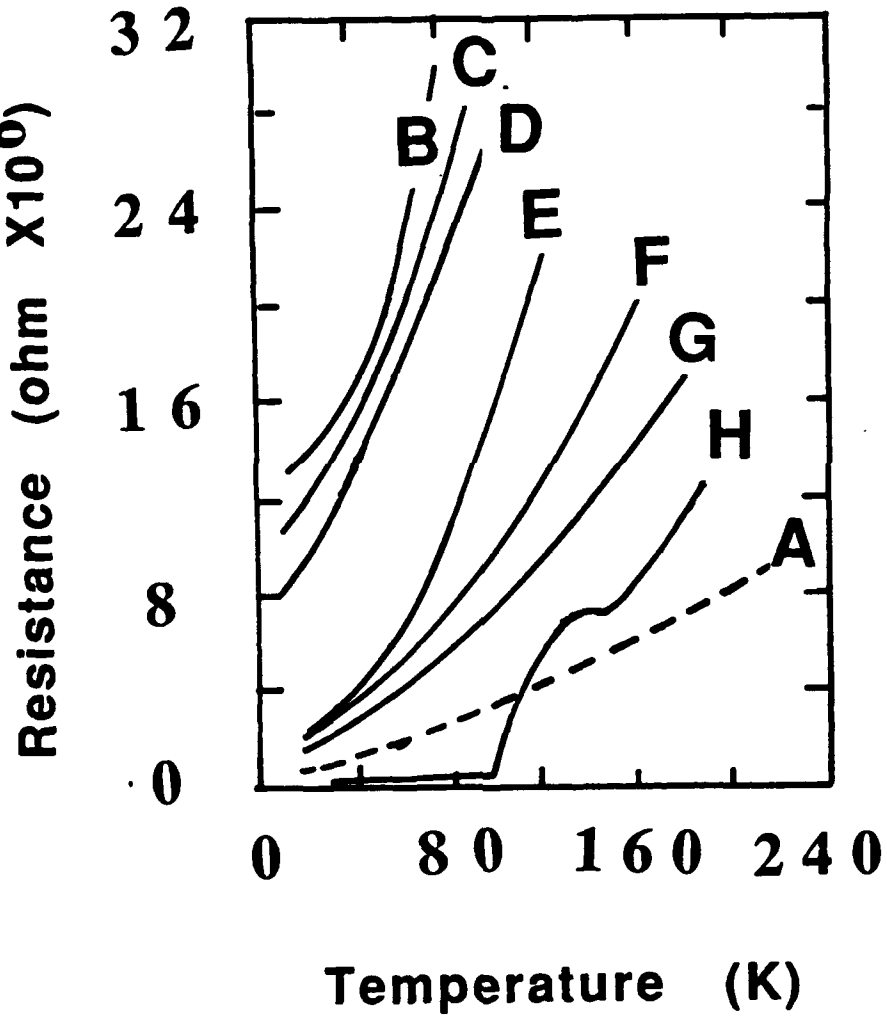

Figure 8. Electrical resistance versus temperature profiles of commercial 1100 grade aluminum and aluminum / $YBa_2Cu_3O_{6+x}$ composites. Aluminum concentration (A) 100, (B) 10, (C) 20, (D) 30, (E) 40, (F) 50, (G) 55 and (H) 60 wt.%.

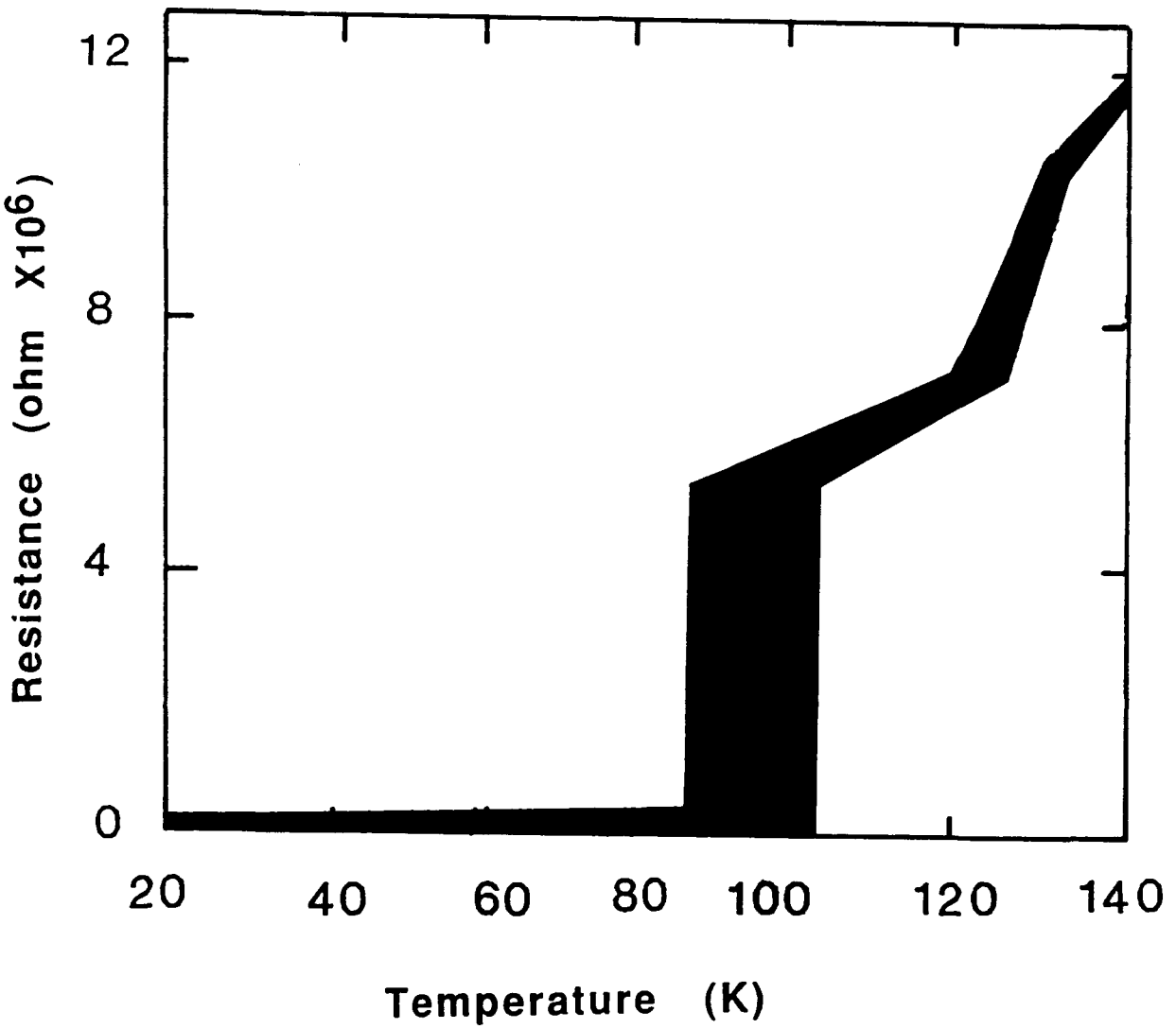

Figure 9. Cumulative plot of the electrical resistance versus temperature profile of 60 wt.% aluminum / 40 wt.% $YBa_2Cu_3O_{6+x}$ composites.

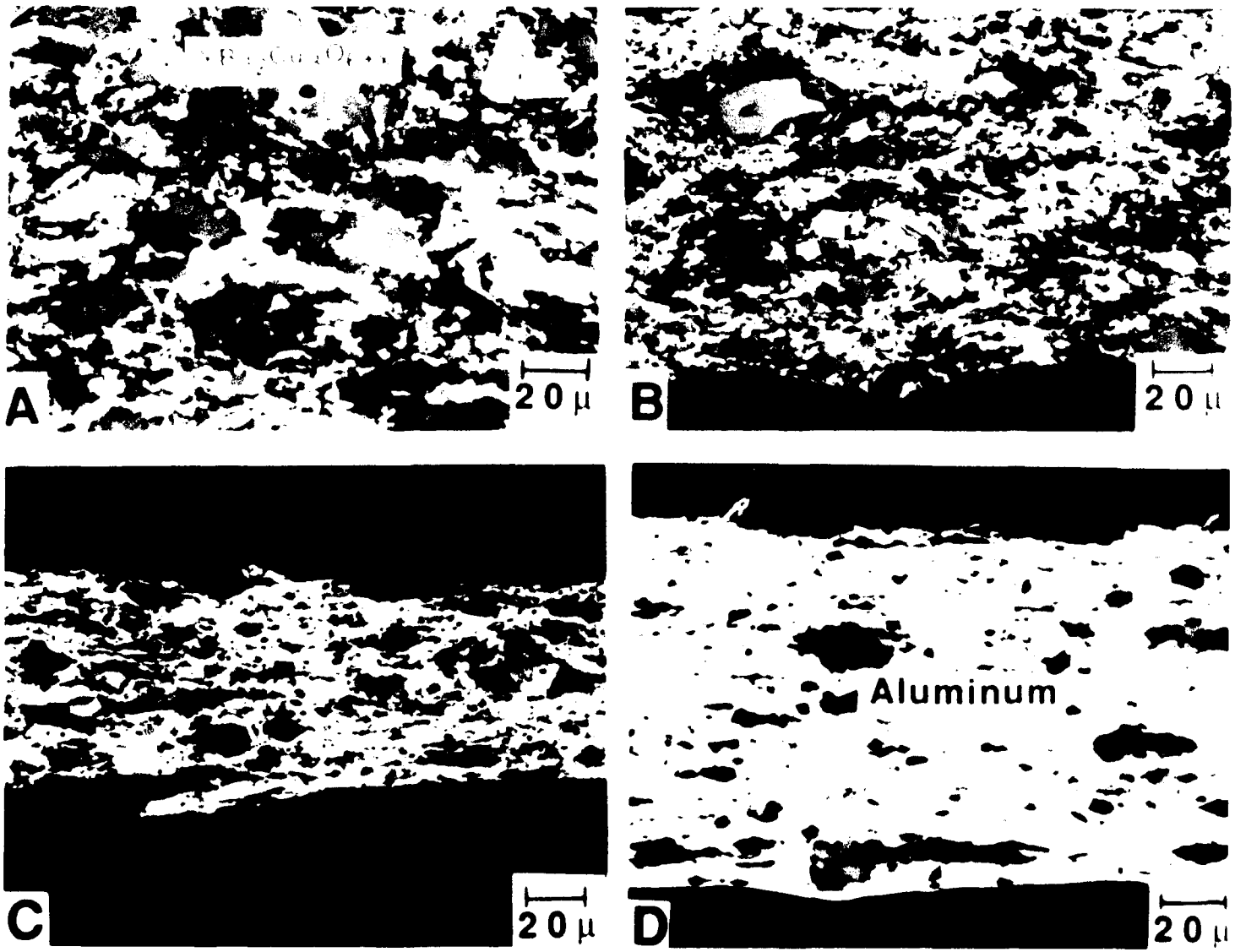

Figure 10. Typical microstructure of polished aluminum / $YBa_2Cu_3O_{6+x}$ composites. Aluminum concentration (A) 10, (B) 20, (C) 40 and (D) 60 wt.%.

very uniform and the degree of uniformity increases with an increase in the concentration of aluminum in the composites.

In order to determine the cohesive strength (that represents the adhesion and bonding of the matrix material and the dispersed superconducting powder) of the hot pressed and cold rolled composites, the bulk composite density was estimated using the water displacement method. The results show that the composite density of all the samples investigated here tends to increases with an increase in the aluminum concentration. However, the hot pressed composite pre-forms containing $\leq$ 40 wt.% aluminum are too fragile and tend to break very easily suggesting that the sintering temperature of 375 - 400^{o}C used in the present processing is not sufficient for the composites containing aluminum < 60 wt.% to sinter and form denser compacts.

In order to reconfirm the observed transitions in the electrical resistance versus temperature profiles of the aluminum/$YBa_2Cu_3O_{6+x}$ composites, a series of additional experiments were conducted and the details of the experiments are as follows :

In the first set of experiments, the electrical resistance of small bars of the composite samples was measured as a function of temperature and applied current. Figure 11 shows typical electrical resistance versus temperature profiles obtained as a function of applied current for 60 wt.% aluminum/40 wt.% $YBa_2Cu_3O_{6+x}$ composites. From a number of such electrical resistance versus temperature measurements, the transition temperatures were determined and the results are shown in Figure 12. The results shown in Figures 11 and

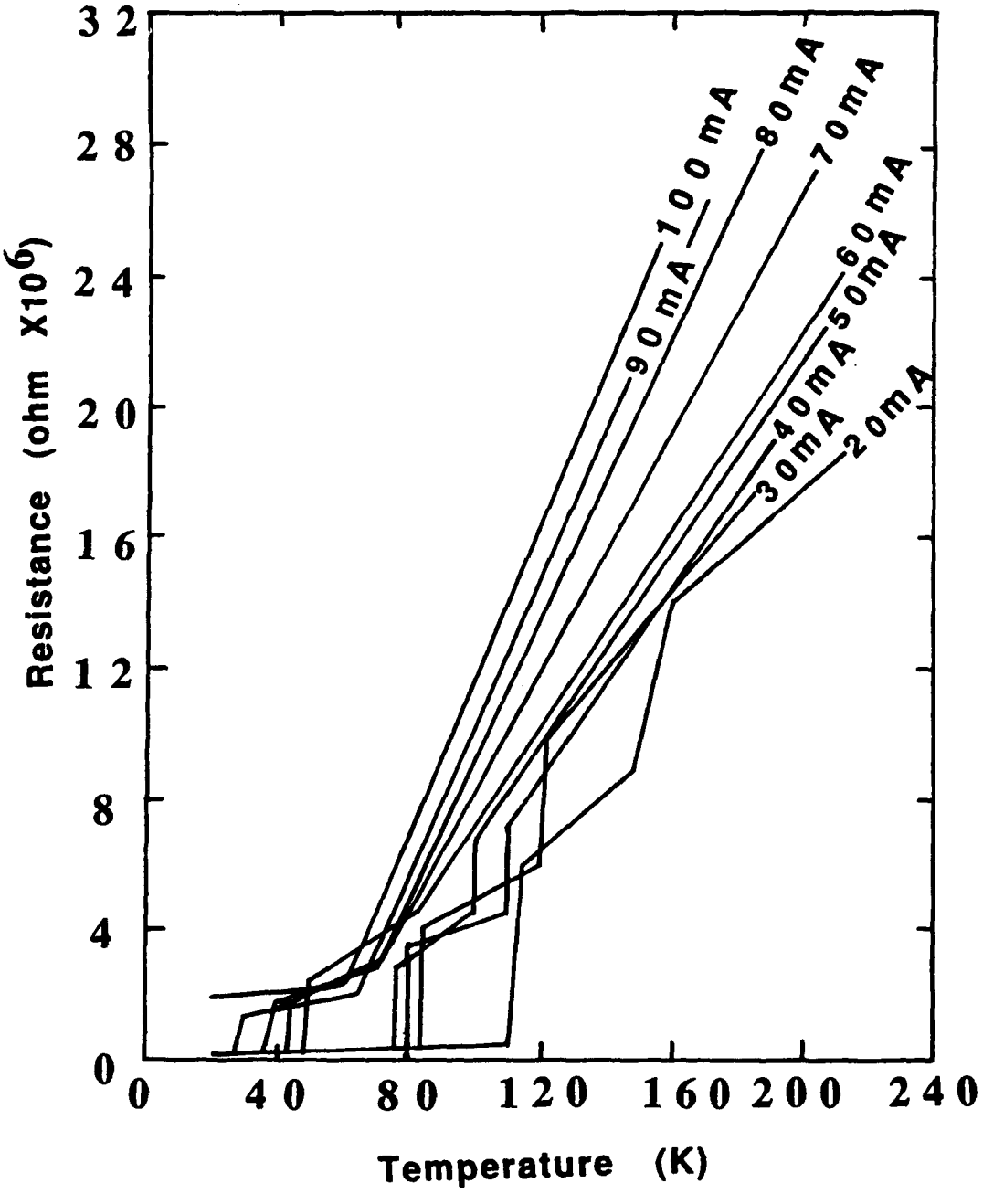

Figure 11. Electrical resistance versus temperature represented as a function of (actual) applied current for 60 wt.% aluminum / 40 wt.% $YBa_2Cu_3O_{6+x}$ composites.

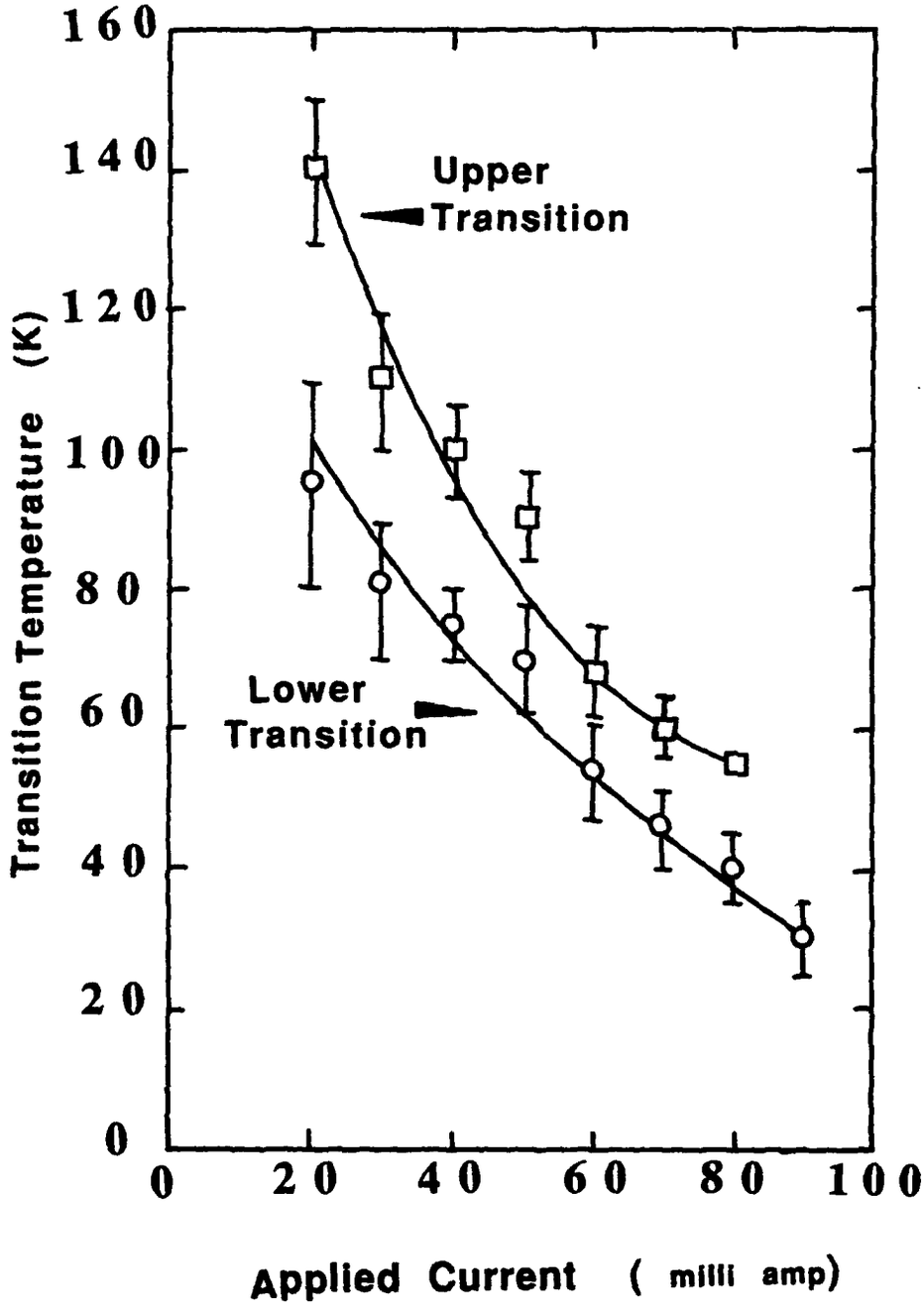

Figure 12. Transition temperature versus (actual) applied current plots of 60 wt.% aluminum / 40 wt.% $YBa_2Cu_3O_{6+x}$ composites.

12 suggest that as the applied current is increased, the transition that was observed in these composites tend to move towards the lower end of the temperature scale. A continued increase in the applied current from 20 milliamperes to 100 milliamperes leads to (i) the disappearance of the high temperature transition (labeled in Figure 12 as "upper transition"); (ii) a shift in the lower transition temperature towards the lower end of the temperature scale and (iii) the eventual loss of the superconducting property of the aluminum composite; at which point the composite tends to behave as a metallic conductor.

In the second set of experiments the magnetic moment of the 60 wt.% aluminum/40 wt.% $YBa_2Cu_3O_{6+x}$ composites was measured as a function of sample temperature and the applied magnetic field strength. Figure 13 shows typical magnetic moment versus temperature profiles of the 60 wt.% aluminum composites. The results suggest that the composites behave as para-magnetic materials above ~77 K and below 77 K they behave as diamagnetic materials. Since the superconductivity is associated with the diamagnetic components, the above results indicate that the 60 wt.% aluminum conductors have a superconducting transition around 77 K. In addition, the results also suggest that the superconducting transition temperature is independent of the applied magnetic field (range 35 - 175 gauss) investigated here.

In the third set of experiments, a few samples that were processed in different batches were analyzed at both Argonne National laboratory (ANL) and Naval Research Laboratory (NRL) using

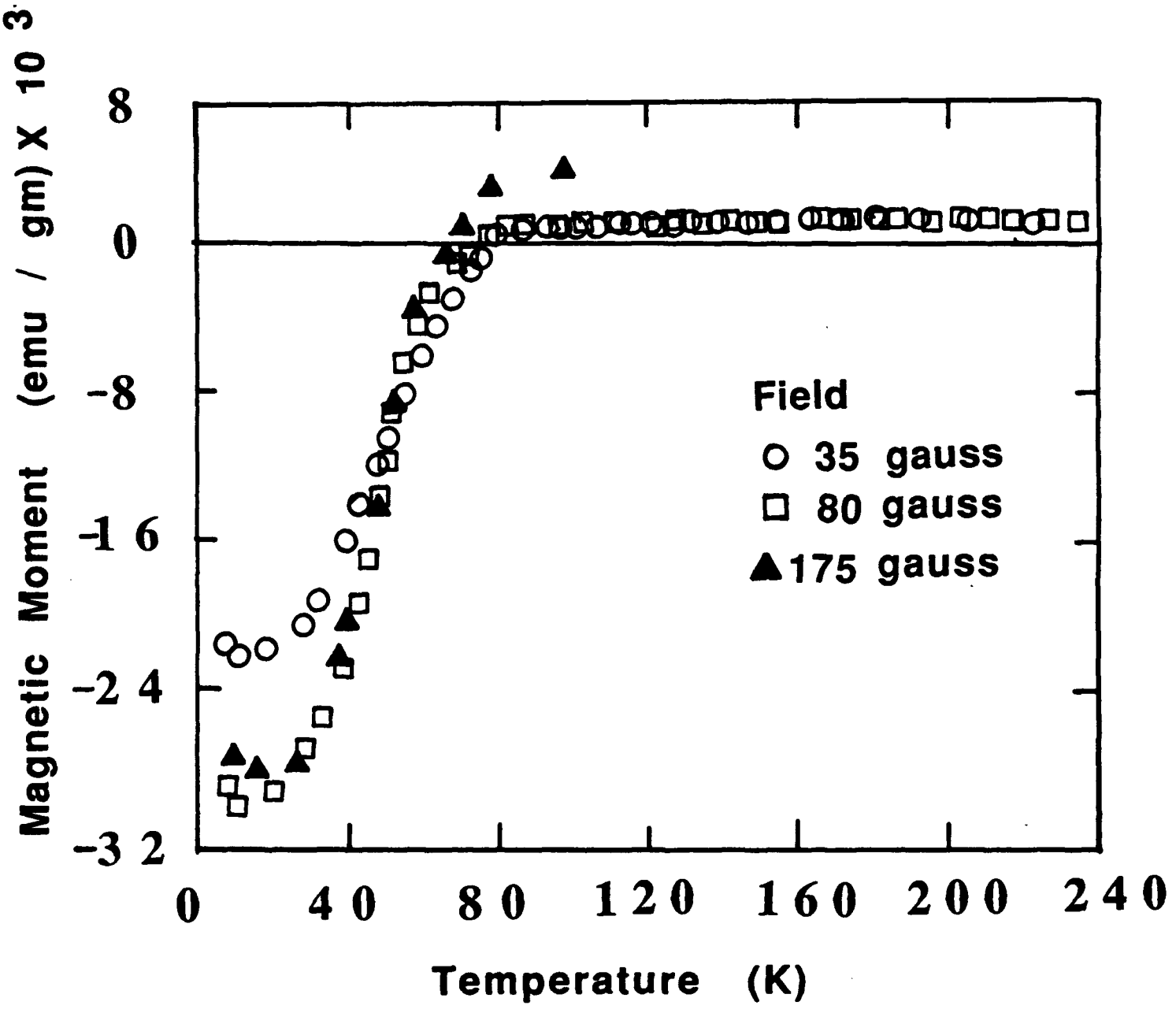

Figure 13. Magnetic moment versus sample temperature profiles of 60 wt.% aluminum / 40 wt.% $YBa_2Cu_3O_{6+x}$ composites measured using SQUID. The applied magnetic field strengths are 35, 75 and 175 gauss.

magnetic susceptibility, four probe DC electrical resistivity and ac susceptibility methods respectively to determine the composite behavior as a function of temperature. Figures 14 - 16 show typical examples of the composite behavior as a function of temperature. The results shown in Figures 14 - 16 indicate that all samples analyzed at both ANL and NRL behave as superconductors above 77 K. However, the samples analyzed at NRL have higher transition temperature.

In the fourth set of experiments, a few samples were sintered at a slightly higher temperature (original sintering temperature was changed from 400°C to 550°C) and a few other samples were sintered at 400°C for a longer time (sintering time was changed from 30 minutes to 120 minutes). Figure 17 shows a typical electrical resistance versus temperature profile of 60 wt.% aluminum/40 wt.% $YBa_2Cu_3O_{6+x}$ composite sintered at 400 and 550°C respectively. The results suggest that the zero resistance transition for this set of test samples sintered at 400°C for 30 minutes occurs around 90 K and a second transition at around 110 K. However, if the composites were sintered at 550°C for 30 minutes or were sintered at 400° for 2 hours, the composites would lose their superconducting property. From the above results it can be inferred that the two new transitions that were observed in 60 wt.% aluminum/40 wt.% $YBa_2Cu_3O_{6+x}$ are very sensitive to the processing parameters, such as sintering temperature and sintering time.

In the fifth set of experiments, a number of samples that represent both thin bars and long wires or tapes were placed in a special sample holder which was mounted in a cryogenic system that

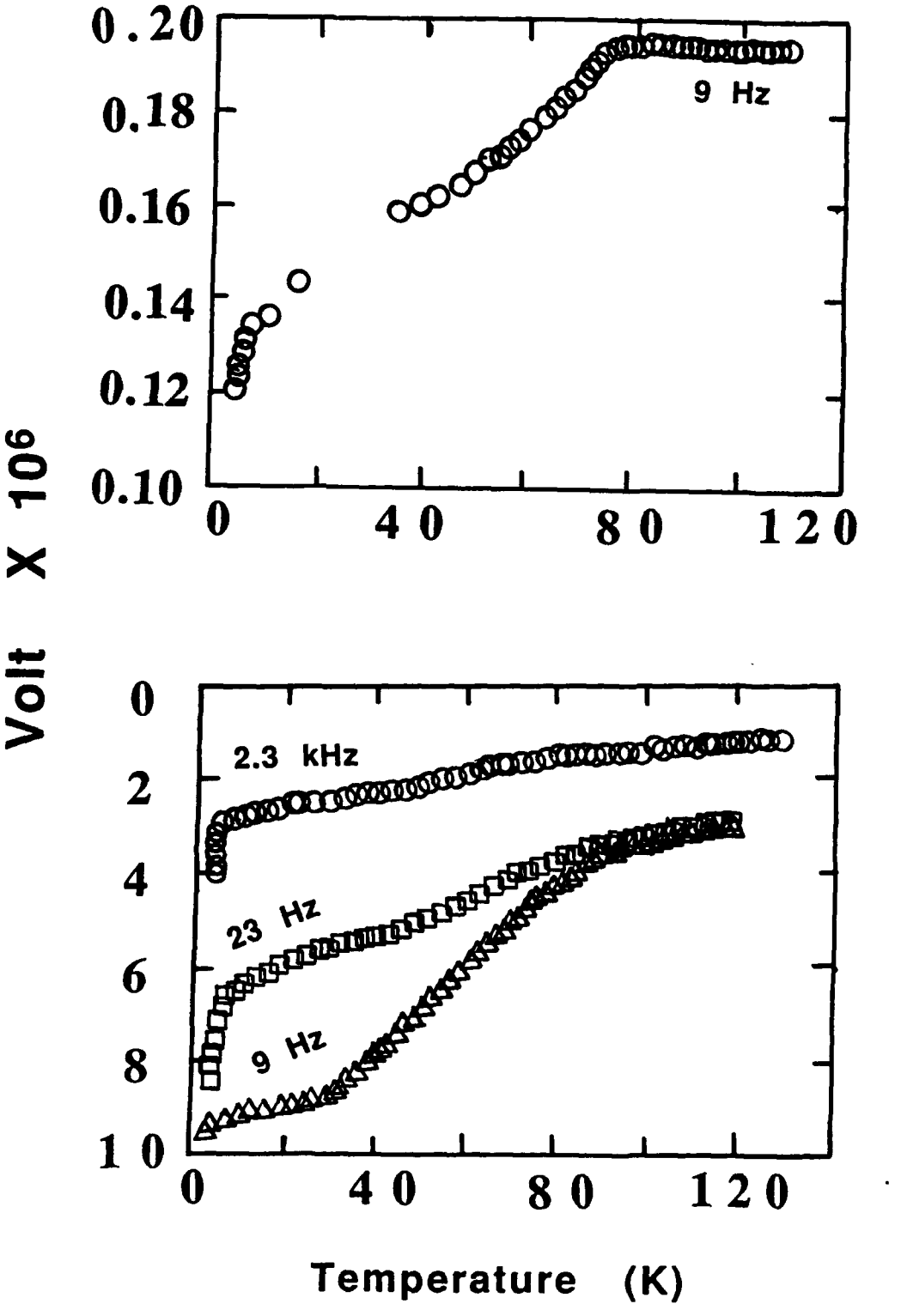

Figure 14. Magnetic susceptibility versus sample temperature profiles of 60 wt.% aluminum/40 wt.% $YBa_2Cu_3O_{6+x}$ composites.

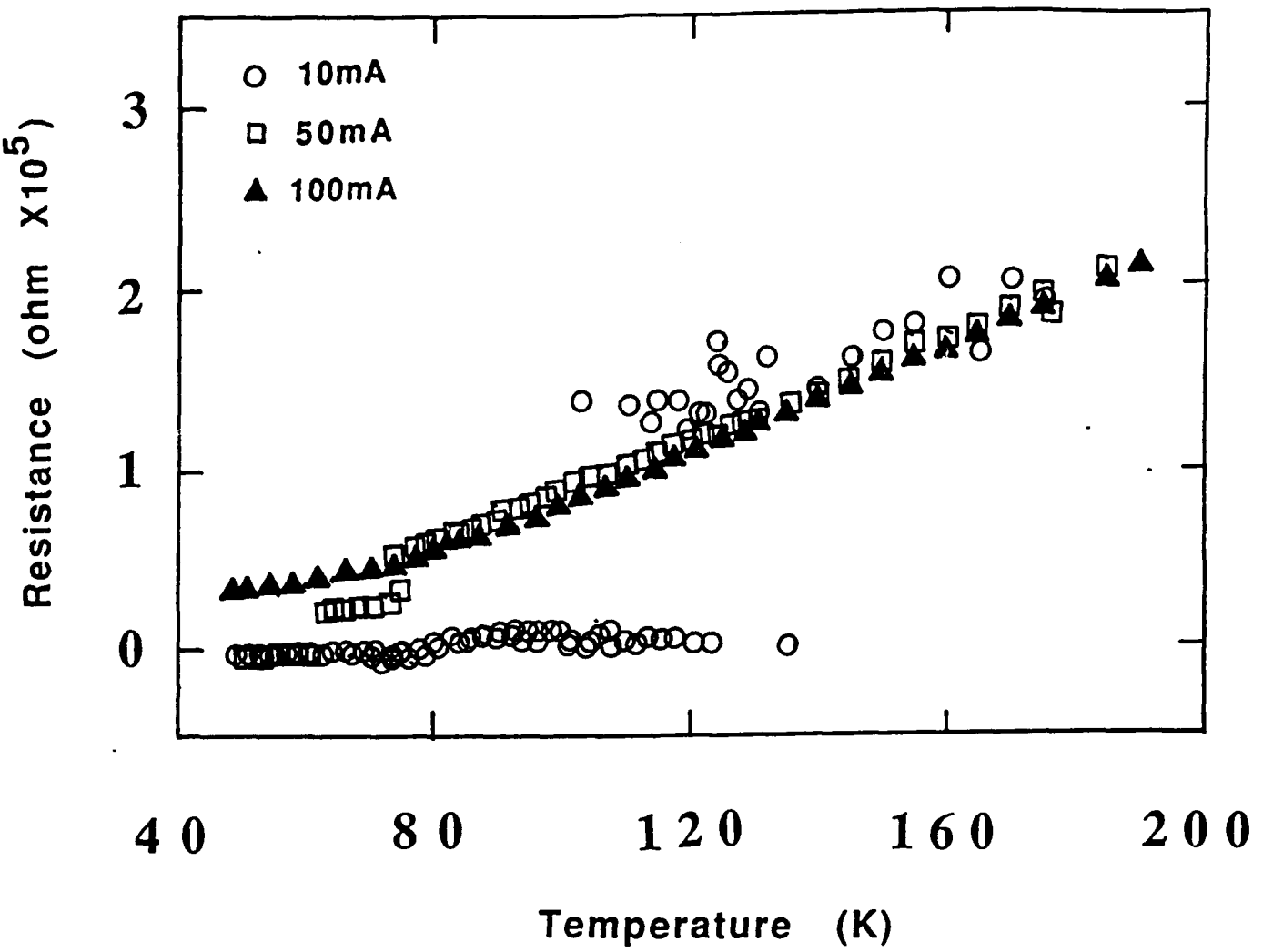

Figure 15. Electrical resistance versus temperature profiles of 60 wt.% aluminum/$YBa_2Cu_3O_{6+x}$ composites.

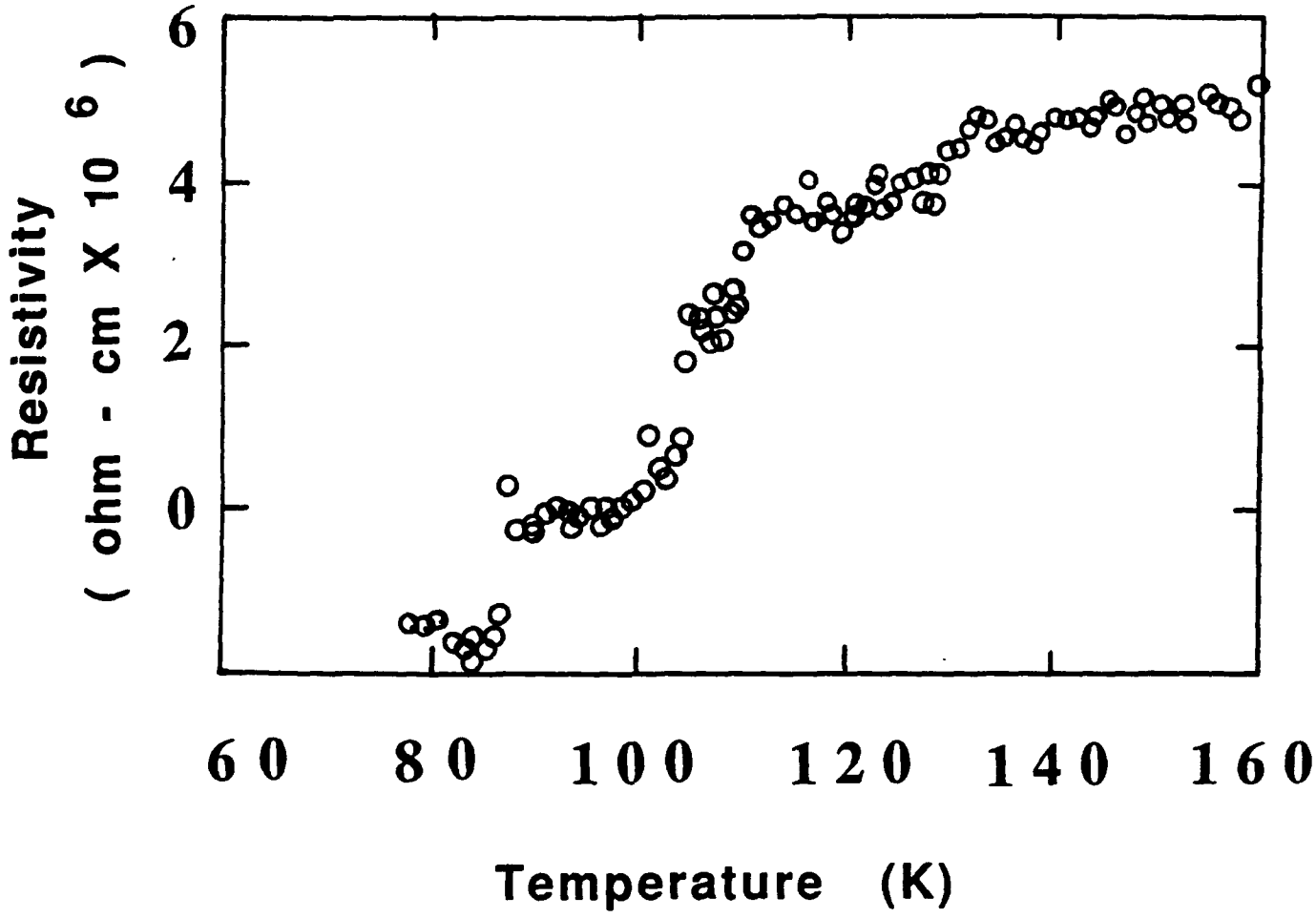

Figure 16. Electrical resistivity versus temperature profiles of 60 wt.% aluminum/$YBa_2Cu_3O_{6+x}$ composites measured using ac susceptibility method.

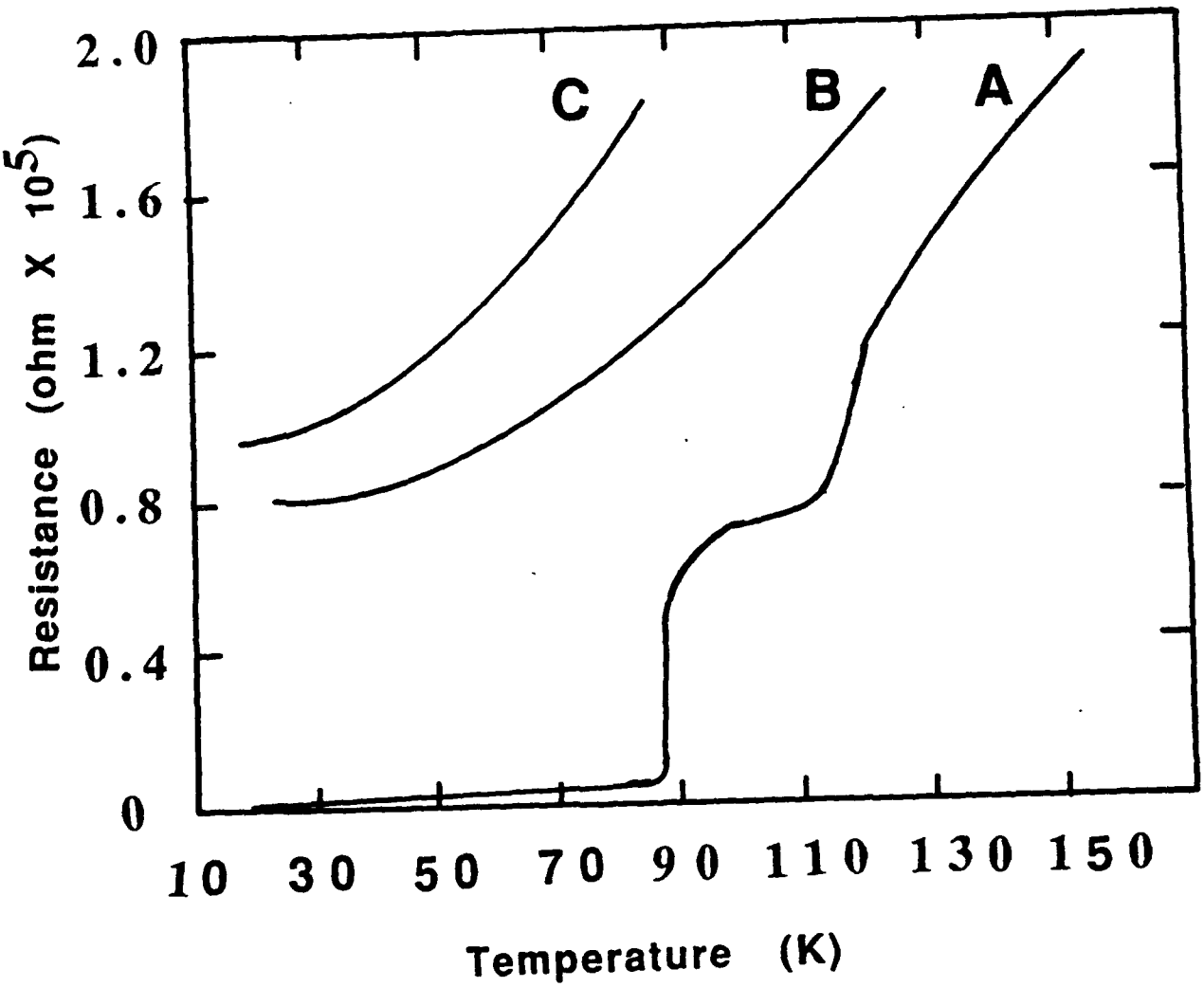

Figure 17. Electrical resistance versus temperature plots of 60 wt.% aluminum / 40 wt. % $YBa_2Cu_3O_{6+x}$ composites represented as a function of (A, C) sintering temperature and (B) duration of sintering. Sintering temperature (A, B) 400°C and (C) 550°C. Duration of sintering (A, C) 30 and (B) 120 minutes.

can be maintained at any temperature in the range of 77 - 300 K. The electrical resistance of the sample was determined as a function of applied current, and the results obtained for a number of measurements made at liquid nitrogen temperature are shown in Figure 18. The results suggest that while the small bar samples can carry current (without offering any resistance) at about 50 amp cm^{-2}, the 50 cm long wires/tapes (wound as coils) can carry currents in the range 10 - 15 amp cm^{-2} respectively. Similar resistance versus applied current measurements obtained for all samples (both small bars and long wires) at room temperature (293 K), in ice (273K) and dry ice (~250K) showed a typical aluminum conductor behavior.

An effort was made to model the aluminum composite system based on the proximity theory, all the efforts failed because the superconducting property of these composites is very unique and is limited to a very narrow concentration range (59 - 61 wt.% aluminum). The mechanism of the observed superconductivity of the 60wt.% aluminum/40 wt.% $YBa_2Cu_3O_{6+x}$ may be explained on the electronic band structure of the composite.

DISCUSSION

The high temperature superconducting ceramic materials are expected to provide a suitable and cost effective alternative to the presently used metallic superconductors, such as NbTi and Nb_3Sn that are being operated at liquid helium temperatures (~4 K). However, for the large scale processing of the ceramic materials into ductile forms remains unresolved. Although, processing via composite fabrication is the possible practical solution to overcome the

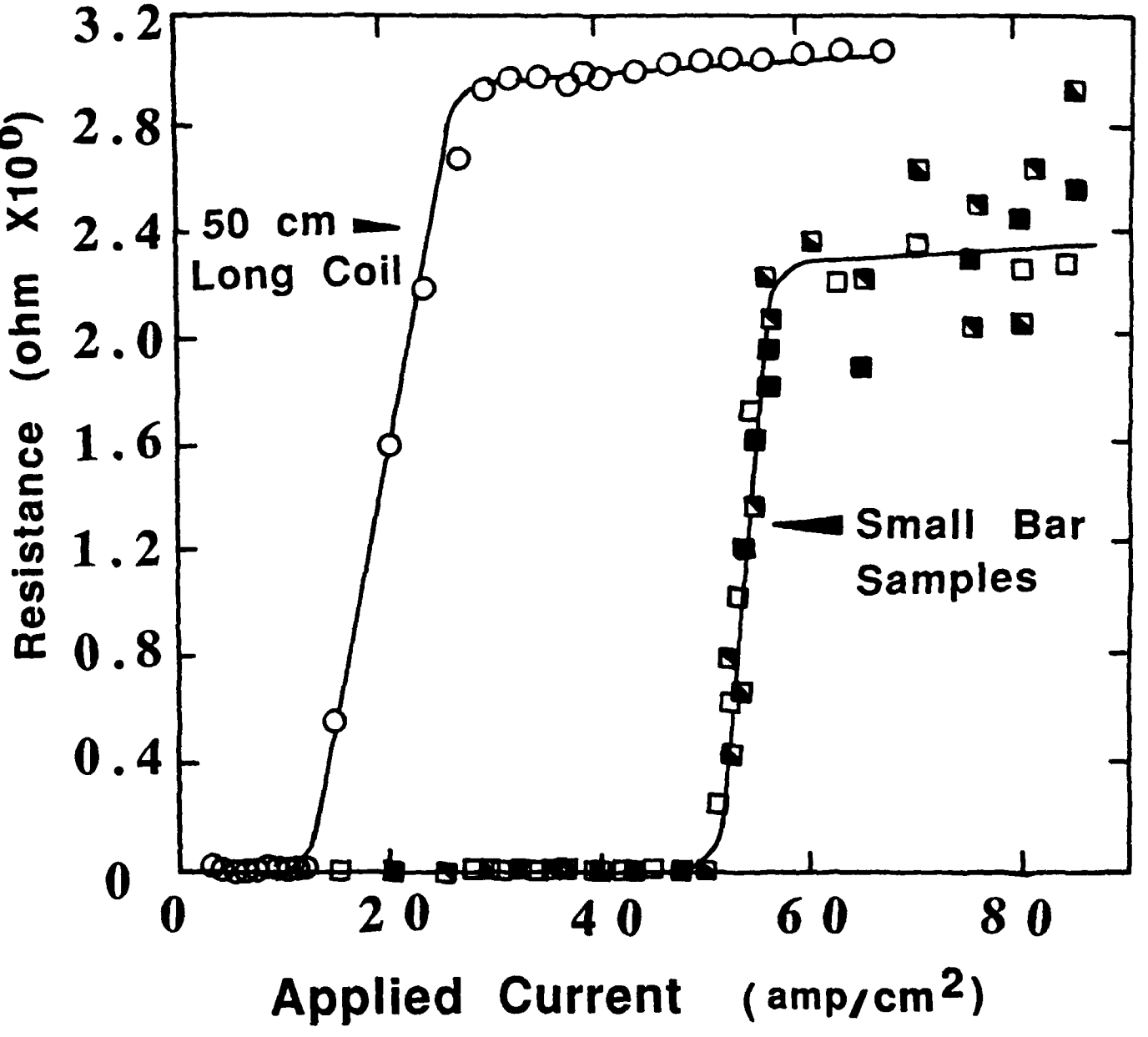

Figure 18. Electrical resistance versus applied current plots of 60 wt.% aluminum / 40 wt.% $YBa_2Cu_3O_{6+x}$ composites measured using (A) small samples and (B) 50 cm long coil at 77K.

brittle nature of the ceramic superconductors, both the superconducting transition temperature (T_c) and the critical current capacity of the ceramic superconductor (J_c) has to maintained. In addition, the added metallic species should not alter the stoichiometry of the superconducting $YBa_2Cu_3O_{6+x}$ ceramic material. Both silver and gold may satisfy all the above requirement, however, based on the economical criteria for large scale manufacturing the noble metal based composite systems are not very practical. Aluminum is a better substitute for the noble metals. It is because (i) the aluminum is readily available and is very cost effective; (ii) from the present investigation it has demonstrated that the new aluminum composite that has been discovered here has a higher superconducting threshold than that of either silver or gold composites. However, it has to be recognized from the present investigation, aluminum based superconducting composite material technology requires further refinement of the processing as well as a better understanding of both the macro- and micro- structural properties of the composites.

The present study indicates that two transitional regions of the resistance versus temperature profile of the aluminum composite exist with the 60 wt.% aluminum/40 wt.% $YBa_2Cu_3O_{6+x}$ composites. However, the physics behind this behavior is not clear. For aluminum composites with $\leq$ 55 wt.% aluminum, it is possible that the present processing conditions (i.e. sintering temperature 400^{o}C, time 30 minutes and uniaxial pressure of 10,000 psi) are (1) not producing dense enough composites and may require higher sintering temperature and/or pressure, and (2) the experimental conditions

tend to accelerate the conversion of aluminum to aluminum oxide in these composites. In order to explore the possibilities additional experiments were conducted. These experiments were the sintering of the composites under 25,000 psi instead of 10,000 psi; the addition of oxygen donating compounds (viz. silver oxide); and the sintering of the composites at a higher temperature in an inert atmosphere. Although, at the present time the experimental results are not very conclusive, it appears that a number of physical variables tend to control the physical behavior of these aluminum composites. For example, (a) the uneven distribution of superconducting $YBa_2Cu_3O_{6+x}$ particles in the matrix of aluminum that results from the extrusion process could be an important factor. Figures 19 (A) and (B) show a typical microstructure of 60 wt.% aluminum composite obtained from two different regions of 50 cm long coil. The results suggest that while the superconducting $YBa_2Cu_3O_{6+x}$ is uniformly distributed in the microstructure representing area (A), large clustering of $YBa_2Cu_3O_{6+x}$ particles is discernible in the microstructure representing the area shown in Figure 19(B). A semi-qualitative estimate of the local composition of the composite indicates that the region shown in Figure 19(B) represents a typical localized concentration of 20 wt.% aluminum and 80 wt.% $YBa_2Cu_3O_{6+x}$ composite. It has been shown in Figure 8 that 20 wt.% aluminum/80 wt.% $YBa_2Cu_3O_{6+x}$ composite does not show the superconducting transition. The net effect of such wire drawing or rolling induced microstructural heterogeneity would degrade the overall superconducting property of the extruded wires or tapes. As a result the overall current carrying capacity of the long coils or

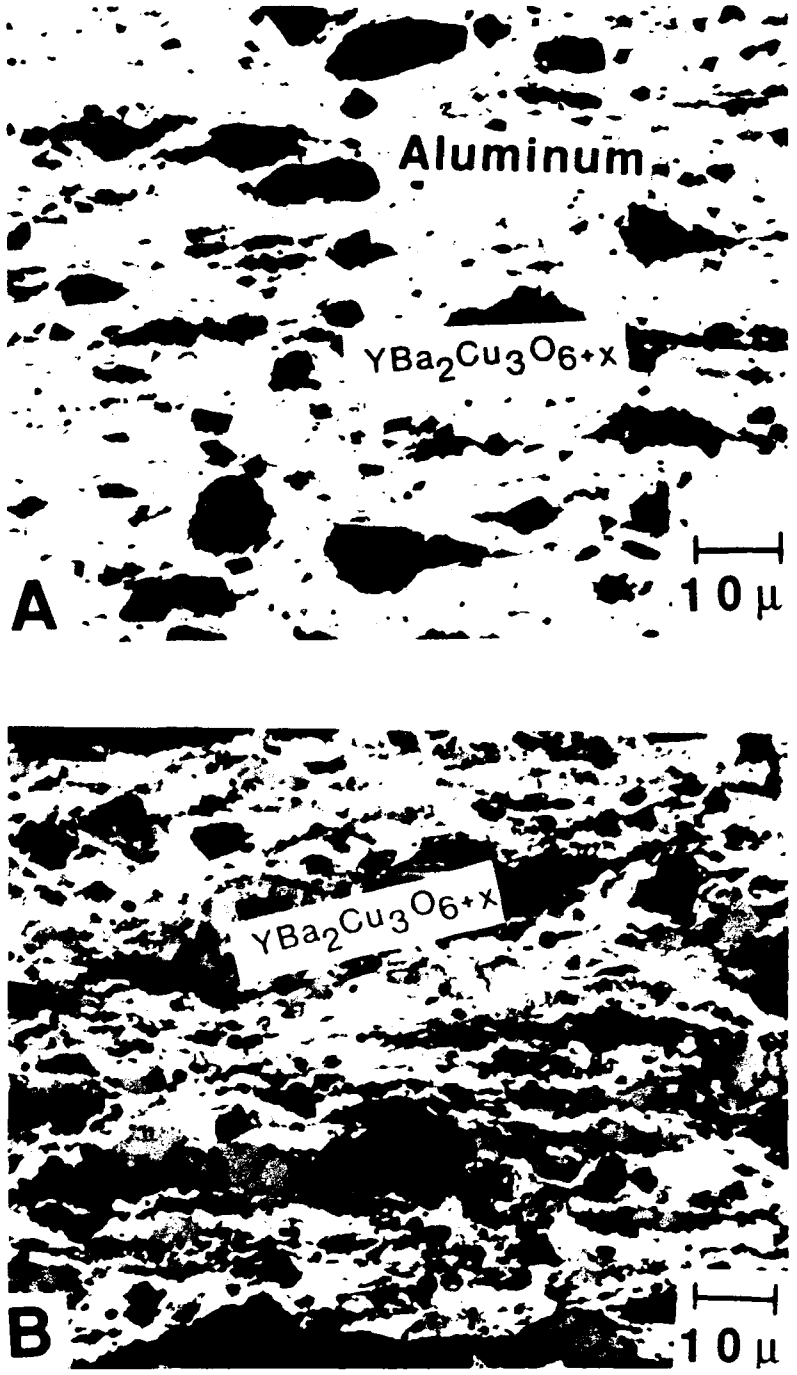

Figure 19. Typical microstructure representing two different regions of the polished surface of a long 60 wt.% aluminum / 40 wt.% $YBa_2Cu_3O_{6+x}$ composite wire. Region (A) represents the uniform distribution of $YBa_2Cu_3O_{6+x}$ and the region (B) represents aggregation of $YBa_2Cu_3O_{6+x}$ particles.

tapes decrease. (b) The experimental results indicate that if the composite contains low levels of aluminum, the aluminum tends to be surrounded by $YBa_2Cu_3O_{6+x}$ and/or the excess CuO particles. As a result, during sintering at 400^oC, the aluminum tends to deplete the free oxygen both from CuO and $YBa_2Cu_3O_{6+x}$ and form aluminum oxide. Figure 20 shows a typical microstructure and the elemental composition of the aluminum matrix, a $YBa_2Cu_3O_{6+x}$ particle and the interfacial region. The results suggest that the composition of the Y-Ba-Cu-O changes from $YBa_2Cu_3O_{6+x}$ to Y_2BaCuO_5 as it approaches close to the interface. Thus the progressional changes can be represented as $YBa_2Cu_3O_{6+x}$ - $YBaCu_2O_{4+x}$ - Y_2BaCuO_5 - $YBaCu_{10}5Al$ - Al. (c) If the aluminum content of the composite is too high, a thin layer (typically 10 - 20 nm and rich in Y_2O_3) tends to form and grow along the perimeter of the $YBa_2Cu_3O_{6+x}$ particles (Figure 21). In order to understand the mechanism of the above mentioned processes, additional experiments will be conducted to relate the microstructure of the composite and the process methodology.

In addition, a theoretical model based on the electronic band structure, Fermi energy of the surface of $YBa_2Cu_3O_{6+x}$ are being explored at the present time in order to understand the effect of the partial diffusion of aluminum into the lattice of $YBa_2Cu_3O_{6+x}$ and / or the presence of aluminum atom close to the lattice of $YBa_2Cu_3O_{6+x}$ on the electronic structure and the hole concentration of the superconductor. The results of both the experimental analysis and predictions of the theoretical model on the electronic structure of $YBa_2Cu_3O_{6+x}$ in presence of aluminum will be presented at a later date.

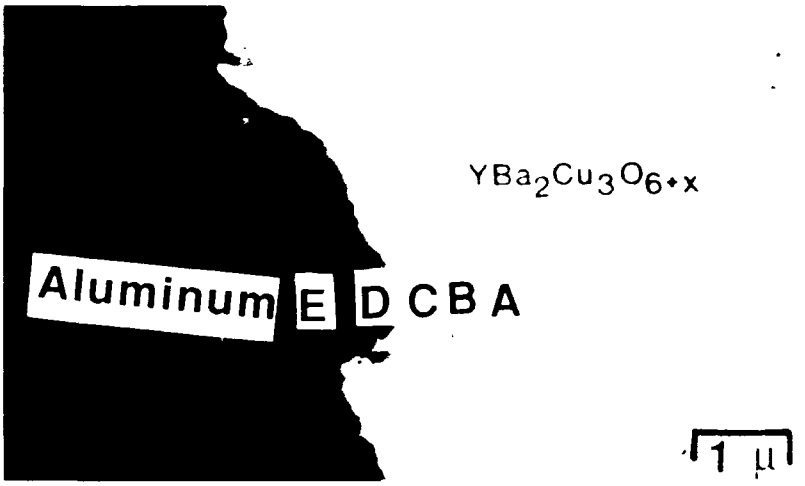

	Elemental Composition (atomic %)				
	Yttrium	Barium	Copper	Aluminum	Others
A	16.08	31.71	48.09	--	4.12
B	19.32	24.61	52.07	--	4.00
C.	50.06	24.19	25.73	--	--
D	6.03	5.69	60.49	27.38	0.43
E	--	--	--	100.00	--

Figure 20. Typical microstructure and the corresponding compositional analysis of $YBa_2Cu_3O_{6+x}$ - aluminum interface.

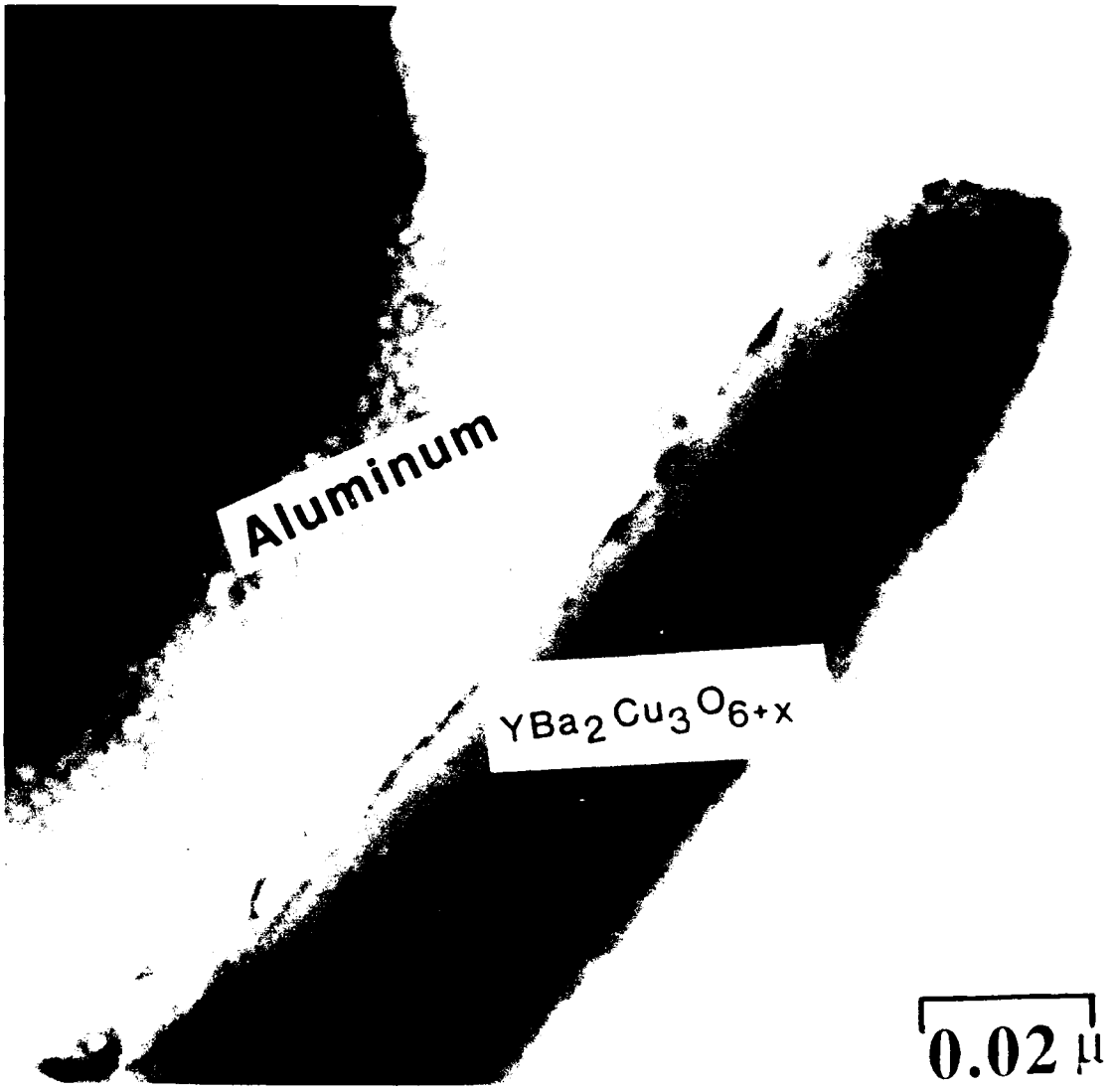

Figure 21. The transmission electron micrographs obtained from the interfacial region between aluminum matrix and $YBa_2Cu_3O_{6+x}$ particle.

CONCLUSION

From the present investigation the following conclusions can be derived :

1. The addition of excess 5 moles of copper to $YBa_2Cu_3O_{6+x}$ does not affect the superconducting behavior of pure $YBa_2Cu_3O_{6+x}$ material. The composition based on excess CuO is more useful and convenient for the large scale processing of the superconducting materials.
2. The addition of silver to the $YBa_2Cu_3O_{6+x}$ does not affect the superconducting behavior of $YBa_2Cu_3O_{6+x}$ over the entire concentration range of 10 - 72 wt.% silver. However the T_c decreases from T_c 77 K to 60 K with an increase in the concentration of silver above 40 wt.% to 72 wt.% (Figure 22).
3. The critical current carrying capacity of silver composites tends to decrease (from 100 to 25 amp cm^{-2}) as a result of the increase in the concentration of silver in the composite (from 10 - 72 wt.%).
4. Although, the theoretical models based on classical proximity theory of low temperature superconductors can predict the lowering of T_c with the increase in the concentration of silver in the composites, the extrapolated length for the diffusion of superconductivity from $YBa_2Cu_3O_{6+x}$ into silver matrix predicted from the theory are not agreeable with the experimentally determined superconducting $YBa_2Cu_3O_{6+x}$ particle - particle separation distance.
5. Aluminum/$YBa_2Cu_3O_{6+x}$ composites behave as superconductors only within a narrow aluminum concentration range (58 - 61 wt.%

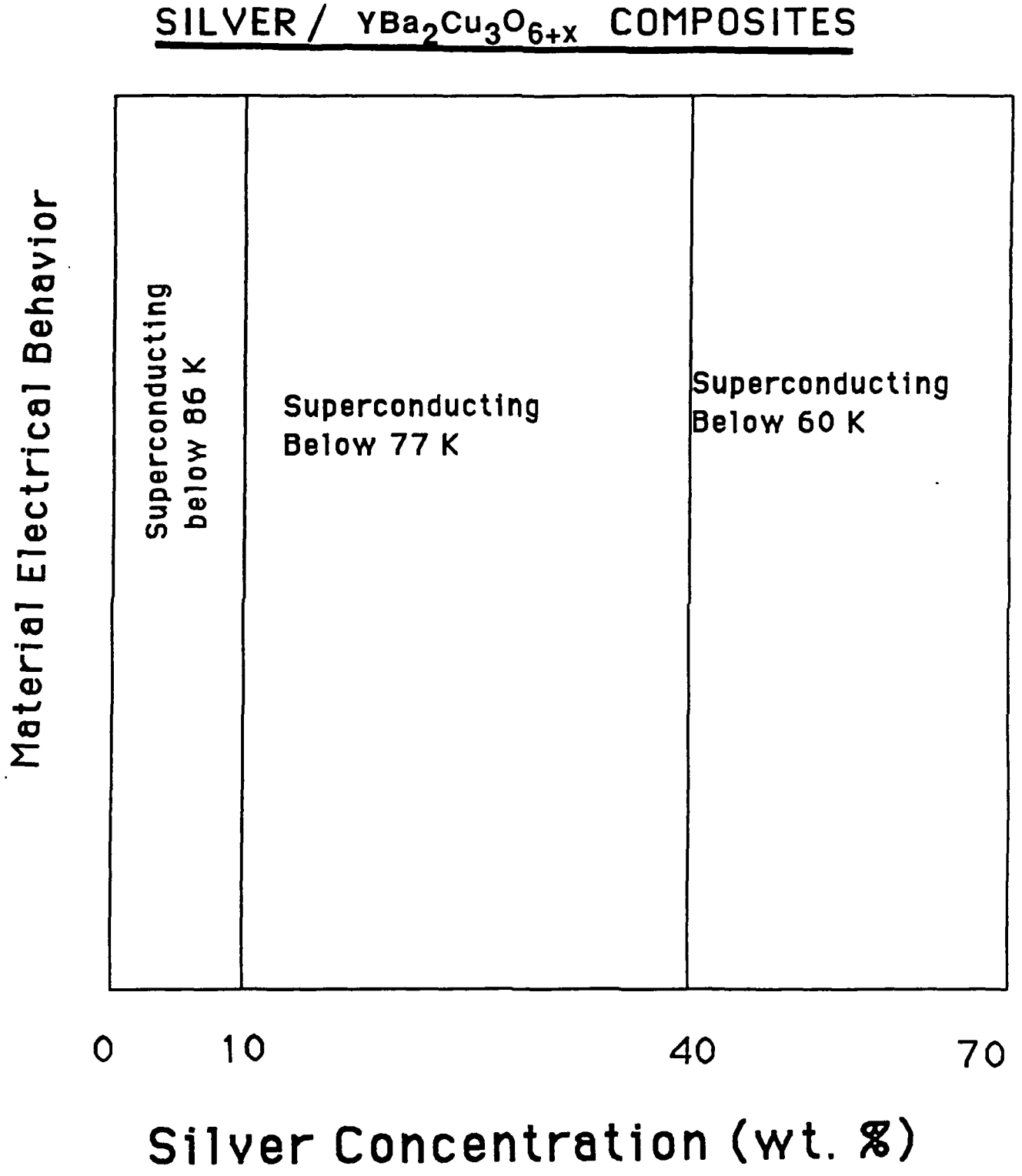

Figure 22. Schematic representation of the material electrical property as a function of silver concentration for silver / $YBa_2Cu_3O_{6+x}$ composites.

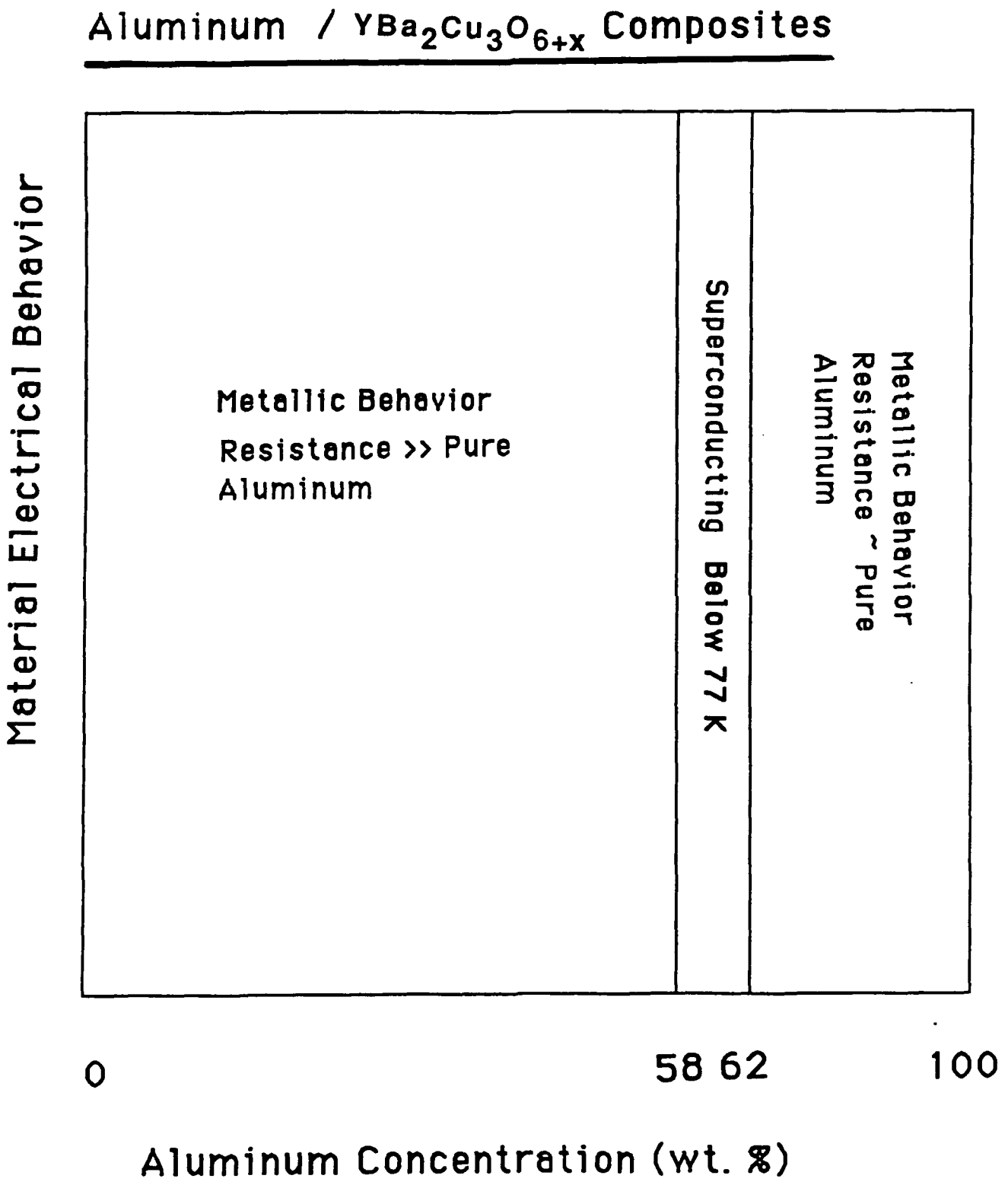

Figure 23. Schematic representation of the material electrical property as a function of aluminum concentration for aluminum / $YBa_2Cu_3O_{6+x}$ composites.

aluminum / 42 - 39 wt.% $YBa_2Cu_3O_{6+x}$ (Figure 23)) and no present theory can explain the mechanism of the superconductivity in these composites.

6. 60 wt.% Aluminum/40 wt.% $YBa_2Cu_3O_{6+x}$ composites show two transitions around 90 and 120 K respectively.
7. The observed transitions strongly depend upon the applied current.
8. The observed transitions are very sensitive to the process parameters such as sintering temperature and the sintering time.
9. Conventional cold rolling of aluminum/$YBa_2Cu_3O_{6+x}$ pre-forms tends to produce tapes or wires with an uneven distribution of superconducting $YBa_2Cu_3O_{6+x}$ phase.
10. The critical current density of small samples, and long wires at liquid nitrogen temperature is about 50 amp cm^{-2} and 10 - 15 amp cm^{-2} respectively.

ACKNOWLEDGMENT

The author would like to thank Drs. O. P. Arora, L. F. Aprigliano, D. R. Ventriglio, A. Purohit (ANL) and C. S. Pande (NRL) for their valuable suggestions and useful discussions.

REFERENCES

1. Bednorz, J. C. and Muller, K., "Possible High T_c Superconductivity in Barium-Lanthanum-Copper-Oxygen System," Z. Phys. B. Condensed matter, 64, 189 (1986).
2. Wu, M. K. et al., "Superconductivity at 93 K in a Mixed Phase of Y-Ba-Cu-O Compound System at Ambient Pressure," Phys. rev. Letts., 58, 908 (1987).
3. Maeda, H., Tanaka, Y., Fukutomi, M. and Asano, T., "A New High T_c Oxide Superconductor without a Rare Earth Element," Jap. J. Appl. Phys., 27(2), 1209 91988).

4. Hepp, A. F., Gaier, J. R., Hambourger, P. D. and Pouch, J. J., "Interaction of Au, Ag, and Bi Ions with $YBa_2Cu_3O_{7-y}$: Implications for Superconductor Applications," Processing and Applications of High T_c Superconductors, edt. W. E. Mayo, Pub. The Metallurgical Society, 213 (1988).

5. Yao, Y. D., etal, "Critical Current Density Enhancement and Moisture Destruction Studies of the Compound Superconductor Y-Ba-Cu-Ag-O," Mat. Res. Soc. Symp. Proc., 99, 407 (1988).

6. Sen, S., In-Gann Chen, Chen, C. H. and Stefanescu, D. M., "Fabrication of Stable Superconductive Wires with $YBa_2Cu_3O_{6+x}$ /Ag_2O Composite Core," Appl. Phys. Letts., 54(8), 766 (1989).

7. In-Gann Chen, Sen. S. and Stefanescu, "Superconductive Aluminum / $YBa_2Cu_3O_{6+x}$ Composites Stabilized by Oxygen/Fluorine Donors," Appl. Phys. Lett., 52, 1355 (1988).

8. Frank, J. P., Jung, J. and Mohammed, M. A. K., "Superconductivity in the System (Al_xY_{1-x}) $Ba_2Cu_3O_{6.5+z}$," Phys. Rev. B., 36, 2308 (1987).

9. Siegrist, T., et al., "Aluminum Substitution in $YBa_2Cu_3O_7$," Phys. Rev. B., 36, 8365 (1987).

10. Zhao, Y., Liu, H. K. and Dow, S. X., "Effect of co-doping of Ca and Al on the Hole Concentration and Superconductivity in the $YBa_2Cu_3O_{7-y}$ System," Physica C, 179, 207 (1991).

11. Jin, S., "Processing Techniques for Bulk High T_c," J. Metals, 43(3), 269 (1991).

12. Rao, A. S., Aprigliano, L. F. and Arora, O. P., US Patent 4,983,571 (1990).

13. Deutscher, G., and de Gennes, P. G.., "Proximity Effects," in Superconductivity, edt. Parks, R.D., Pub. Macel Dekker, Inc., New York, NY, 2, 1005 (1969).

14. Pande, C. S., Private Communication.

15. Rao, A. S., Aprigliano, L. F. and Arora, O. P., "Effect of the Additives on Morphology and Superconductivity of $YBa_2Cu_3O_{6+x}$ Ceramic materials," Bull. Mater. Sci., 14(2), 269 (1991).

16. In-Gann Chen, Sen. S. and Stefanescu, D. M., "Production of Stabilized Superconducting Metal/$YBa_2Cu_3O_x$ Composites by Conventional Metallurgical Techniques," High T_c Superconductors, edt. W. E. Mayo, Pub. The Metallurgical Society, 151 (1988).

DISTRIBUTION

Copies

1 NRL Code 6000 (Rath)

5 DTIC

CENTER DISTRIBUTION

Copies	Code	Name
1	28	(Wacker)
1	281	(Holsberg)
1	283	(Singerman)
1	284	(Fischer)
1	2801	(Ventriglio)
1	2802	(Morton)
1	2803	(Cavallaro)
1	2809	(Malec)
1	2812	(Arora)
5	2812	(Rao)
1	2813	(Ferrara)
1	2814	(Montemarano)
1	2815	(DeNale)
1	0113	(Douglas)
1	522.1	TIC (C)
1	522.2	TIC (A)
1	5231	Office Services

REPORT DOCUMENTATION PAGE

Form Approved
OMB No. 0704-0188

Public reporting burden for this collection of information is estimated to average 1 hour per response, including the time for reviewing instructions, searching existing data sources gathering and maintaining the data needed, and completing and reviewing the collection of information. Send comments regarding this burden estimate or any other aspect of this collection of information, including suggestions for reducing this burden, to Washington Headquarters Services, Directorate for information Operations and Reports, 1215 Jefferson Davis Highway, Suite 1204, Arlington, VA 22202-4302, and to the Office of Management and Budget, Paperwork Reduction Project (0704-0188), Washington DC 20503

1. AGENCY USE ONLY (Leave blank)	2. REPORT DATE	3. REPORT TYPE AND DATES COVERED
	01 Jan 1993	

4. TITLE AND SUBTITLE
Processing and Property Evaluation of Silver or Aluminum Matrix $YBa_2Cu_3O_{6+x}$ Superconducting Materials

5. FUNDING NUMBERS
Work Unit No.
1-2812-148

6. AUTHOR(S)
A. Srinivasa Rao

7. PERFORMING ORGANIZATION NAME(S) AND ADDRESS(ES)
Naval Surface Warfare Center
Carderock Division
Annapolis Detachment
Annapolis, MD 21402-5067

8. PERFORMING ORGANIZATION REPORT NUMBER
CARDEROCKDIV-SSM-61-93/05

9. SPONSORING / MONITORING AGENCY NAME(S) AND ADDRESS(ES)
Office of Naval Research
CDNSWC - IR Program
Annapolis, Maryland 21402-5067

10. SPONSORING / MONITORING AGENCY REPORT NUMBER

11. SUPPLEMENTARY NOTES

12a. DISTRIBUTION / AVAILABILITY STATEMENT
Unlimited

12b. DISTRIBUTION CODE

13. ABSTRACT *(Maximum 200 words)*

In order to understand the physical behavior at the atomistic level of the superconducting metal matrix composites, both aluminum/$YBa_2Cu_3O_{6+x}$ and silver/$YBa_2Cu_3O_{6+x}$ composites have been investigated. The results suggest that silver forms superconducting composites in the concentration range 10-72 wt. %. The aluminum based composites showed the superconducting property only for composites containing 60 wt.% aluminum and 40 wt. % $YBa_2Cu_3O_{6+x}$. In addition, it was found that the superconducting behavior of the aluminum $YBa_2Cu_3O_{6+x}$ composites is very sensitive to the sintering temperature and the duration of sintering.

14. SUBJECT TERMS
Processing, Silver, Aluminum, Superconductivity

15. NUMBER OF PAGES

16. PRICE CODE

17. SECURITY CLASSIFICATION OF REPORT	18. SECURITY CLASSIFICATION OF THIS PAGE	19. SECURITY CLASSIFICATION OF ABSTRACT	20. LIMITATION OF ABSTRACT
Unclassified	Unclassified	Unclassified	